Water Balance Modelling of the Tandjari Reservoir in Burkina Faso

Master of Science Thesis

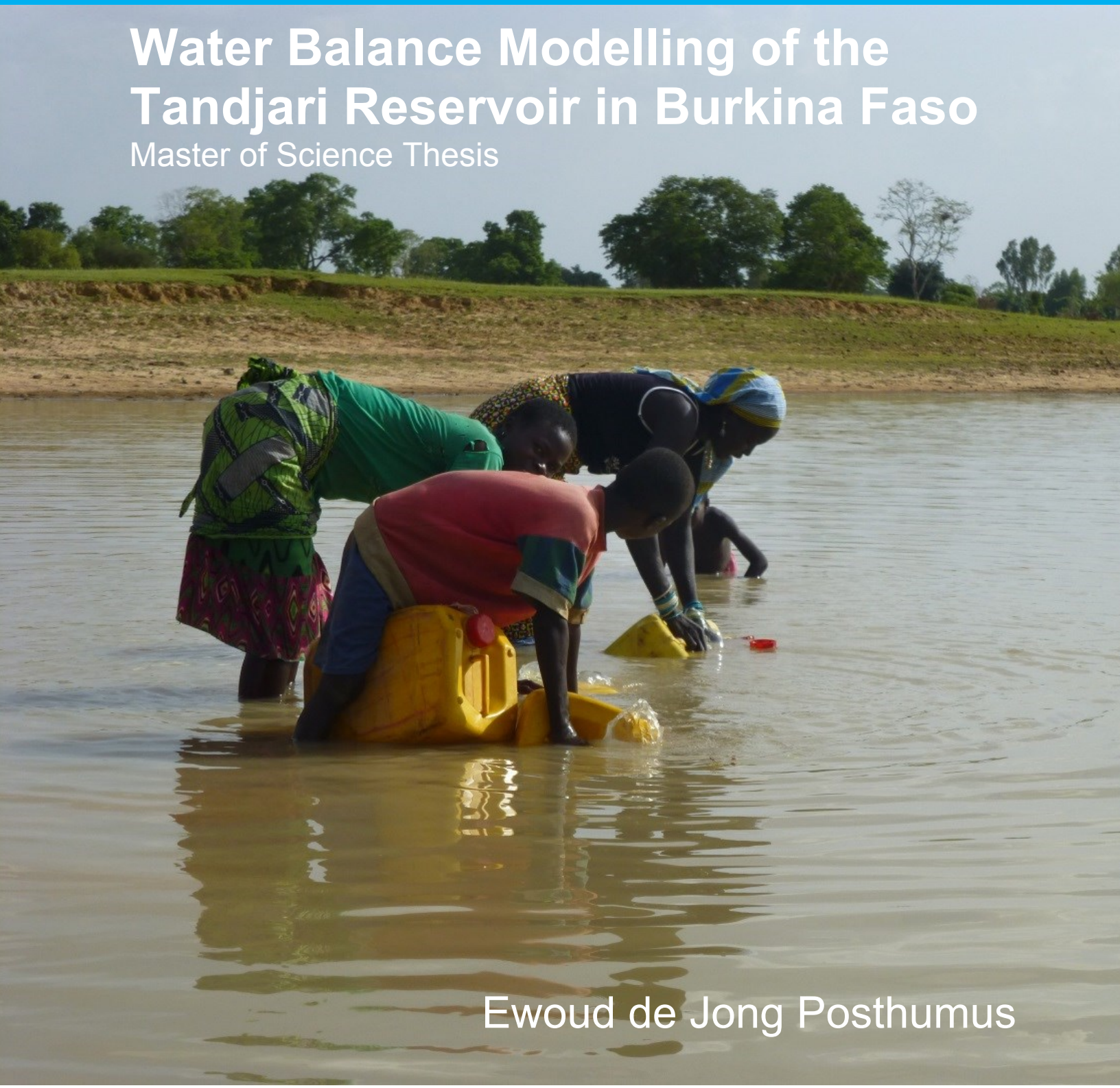

Ewoud de Jong Posthumus

Universiteit Utrecht

The photo on the cover page shows women filling up their jerrycans with water from the Tandjari reservoir. The photo was taken by the author on June 1, 2016.

Water Balance Modelling of the Tandjari Reservoir in Burkina Faso

For the degree of Master of Science
Water Science and Management at Utrecht University

Jong Posthumus, E.C. de (Ewoud)

March 2017

Graduation Committee

dr. P.P. Schot (Utrecht University)
dr. Aat Barendregt (Utrecht University)
J. Stoffels MSc. (World Waternet)

Faculty of Geosciences · Utrecht University

This research was made possible by
World Waternet
Agence de l'Eau du Gourma

Universiteit Utrecht

Abstract

The construction of reservoirs is a widely used strategy for dealing with limited water availability by capturing runoff. In Burkina Faso reservoirs supply water for; irrigation in agriculture and for both human consumption and livestock. Despite reservoirs being used for a century in Burkina Faso, data on the water balance of reservoirs and their upstream catchments is scarce and knowledge of the importance and applicability of these data is insufficient. In addition, increasing water demands and climate change are calling upon adequate statistics with regard to water availability in reservoirs.
Determining the reservoir water balance and enhancing knowledge on relevant input parameters for a hydrologic model, trend analysis of water utilization, and the impact of possible climatic and water demand changes have been the main goals of this research.

This study focused on the Tandjari reservoir, located in southeast Burkina Faso, for which the various components of the water balance were determined. The reservoir water balance describes the change in water storage, which is dependent on rainfall runoff, groundwater inflow, rainfall on the water surface, evaporation, water consumption, discharge and infiltration into the reservoir bottom. The distributed hydrologic model “Soil and Water Assessment Tool” (SWAT) was used to simulate the water balance components over time. The water balance was simulated for the past five years (2012-2016) and for a future period of ten years (2037-2047). The latter was based on climate and water demand scenarios. Model calibration and validation were based on observed reservoir storage (2012-2016), and uncertainties in model output were quantified using the program “Sequential Uncertainty Fitting Algorithm” (SUFI-2).

The calibration showed that the best simulation fitted the observed storage generally well. 62% of the simulated reservoir storage was within the 95 Percent Prediction Uncertainty (PPU) band. The quality of the model, indicated by the thickness of the 95PPU band and referred to as the R-factor, was 0.49 (out of a perfect 0 and quite reasonable around 1). The acceptable model performance is reflected by the values of the Kling-Gupta efficiency (KGE) and the coefficient of determination (R^2), which were respectively 0.83 and 0.70. The PBIAS value of -0.0 % indicated that the model did not over- or underestimate the observed reservoir storage. Validation of the model, for which a different dataset was used, showed that the 95PPU band bracketed 75% of simulated data and the thickness of the band, indicated by the R-factor, was 0.44. The KGE and R^2 for the validation period (May 2017 to December 2017) were respectively 0.78 and 0.93. The improved behavioral parameters for the validation indicate that the model reliability improved by using a dataset that was obtained from a weather station, which had a better location with respect to the catchment. Moreover the observed reservoir data used in the validation procedure were obtained by automated water level recordings instead of manual readings, which minimized bias due to human intervention.

The water balance, modelled over a period of five years (2012-2016), showed that more than half of the annual reservoir outflow evaporated, about a quarter infiltrated, and less than one-fifth of the total outflow was used for consumption. Infiltration does not need to be considered as direct loss, since nearby villages with wells are likely to benefit from the

infiltration, which ensures year-round groundwater recharge. About 1.4 million cubic meters (MCM) of water is annually infiltrating, however, no conclusions can be drawn on how much of this quantity is actual accessible by groundwater abstraction. The general trend in reservoir water utilization was that by far most water was withdrawn by the drinking water company for the water supply to the people in Fada N'Gourma, followed by irrigation water for agriculture and finally water withdrawals by local residents and livestock. The reservoir was not over-allocated or under stress. The final-to initial-volume ratios, indicate the reservoir is not emptying; hence water is withdrawn from the reservoir at a sustainable rate. At the minimum observed level, the reservoir's capacity was reduced with about 70%, which was enough to sustain important activities including fishing. However, climate change and increasing water demands ask for careful monitoring of the water balance. As water demand gets doubled by 2030, it is expected that during a period of drought the reservoir cannot meet the water demand with the risk that the reservoir empties during the dry season. Climate change could have a worsening effect if the frequency and intensity of droughts will increase. The interruption of water withdrawals over a long period will adversely affect local residents who are depended on this resource.

The results of this study highlight the importance of data collection and analysis, in order to gain understanding of the reservoir behavior and its adjacent catchment in a hydrological context. The quantification of the water balance components is an important task for water management authorities because; it will support the development of operational strategies for water supply and water allocation, it also offers support to the design and implementation of water policy.

Keywords: Reservoir, Water balance, Modelling, Water use, Scenario analysis, Burkina Faso

Résumé

La construction de réservoirs est une stratégie largement utilisée pour faire face à la disponibilité limitée en eau en capturant le ruissellement. Au Burkina Faso, les réservoirs fournissent en eau pour l'irrigation, pour l'agriculture et l'approvisionnement en eau pour les personnes et le bétail. Bien que les réservoirs aient été utilisés pendant un siècle au Burkina Faso, les données sur le bilan de l'eau des réservoirs et leurs bassins versants en amont sont rares et le savoir-faire de la valeur et de l'applicabilité des données est insuffisant. En outre, la demande croissante d'eau et le changement climatique font appel à des statistiques adéquates sur la disponibilité en eau dans les réservoirs.

Les principaux objectifs de cette recherche ont été de déterminer le bilan d'eau du réservoir et d'améliorer les connaissances sur les paramètres d'entrée pertinents pour un modèle hydrologique, l'analyse des tendances de l'utilisation de l'eau et l'impact des changements climatiques et de la demande en eau.

Cette étude a porté sur le réservoir de Tandjari, situé dans le sud-est du Burkina Faso, pour lequel les différentes composantes du bilan d'eau ont été déterminées. Le bilan d'eau du réservoir décrit le changement dans le stockage de l'eau, qui dépend de l'écoulement du

ruissellement, de l'afflux d'eau souterraine, des précipitations sur la surface d'eau, de l'évaporation, de la consommation d'eau, de la décharge et de l'infiltration dans le fond du réservoir. Le modèle hydrologique distribué, appelé 'Soil and water Assessment Tool' (SWAT), a été utilisé pour simuler les composantes du bilan d'eau au fil du temps. Le bilan d'eau a été simulé pour cinq ans (2012-2016), à l'exclusion d'une période d'échauffement de deux ans. L'étalonnage et la validation du modèle sont basés sur le stockage observé des réservoirs (2012-2016) et les incertitudes dans le modèle de sortie ont été quantifiées à l'aide du programme 'Sequential Uncertainty Fitting Algorithm' (SUFI-2).
L'étalonnage a montré que la meilleure simulation correspondait bien au stockage observé. 62% des données mesurées de la réserve de réservoir simulée étaient dans la bande de 95PPU, cela permet de valider les processus de mesure utilisés. La qualité du modèle, indiquée par l'épaisseur de la bande de 95PPU et appelée facteur R, était de 0,49 (sur un 0 parfait, mais tout à fait raisonnable autour de 1). La performance du modèle acceptable est reflétée par les valeurs de l'efficacité de Kling-Gupta (KGE) et du coefficient de détermination (R^2), respectivement de 0,83 et de 0,70. La valeur de PBIAS de -0,0% a indiqué que le modèle n'a pas surestimé ou sous-estimé l'entreposage de réservoir observé. La validation du modèle, pour laquelle différents ensembles de données ont été utilisés, a montré que 75% des données simulées étaient croisées par la bande de 95PPU et que l'épaisseur de la bande, indiquée par le facteur R, était de 0,44. Le KGE et le R^2 pour la période de validation (mai 2017 à décembre 2017) étaient respectivement de 0,78 et 0,93. Les paramètres comportementaux améliorés pour la validation indiquent que la fiabilité du modèle s'est améliorée en utilisant un ensemble de données obtenu à partir d'une station météorologique qui avait un meilleur emplacement par rapport au bassin versant. De plus, les données sur les réservoirs observées utilisées dans la procédure de validation ont été obtenues par des enregistrements automatisés au lieu des lectures manuelles, ce qui a permis de minimiser le biais d'erreur dû à l'intervention humaine.

Le bilan d'eau, modélisé sur une période de cinq ans (2012-2016), a montré que plus de la moitié de la sortie annuelle des réservoirs s'évaporait, environ un quart infiltré et moins d'un cinquième pour la consommation. L'infiltration n'a pas besoin d'être considérée comme une perte directe, puisque les villages voisins avec des puits sont susceptibles de bénéficier de l'infiltration, ce qui assure la recharge des eaux souterraines toute l'année. Environ 1,4 MCM d'eau s'infiltre chaque année, mais on ne peut tirer aucune conclusion quant à la quantité réelle de cette quantité accessible par captage d'eau souterraine. La tendance générale à l'utilisation de l'eau dans les réservoirs a été que la plupart des eaux ont été pompées par l'entreprise d'eau potable pour alimenter les populations de Fada N'Gourma, suivies par l'eau d'irrigation pour l'agriculture et enfin les prélèvements d'eau par les habitants vivant au bord de l'eau du barrage et le bétail. Le réservoir n'a pas été sur-alloué ou stressé. Les rapports du volume final-au-volume-initial indiquent que le réservoir ne se vide pas; par conséquent, l'eau est retirée du réservoir à un taux soutenable. Au niveau minimum observé, la capacité du réservoir a été réduite d'environ 70%, ce qui a suffi à soutenir d'importantes activités, y compris la pêche.

Toutefois, le changement climatique et la demande croissante en eau demandent un suivi attentif du bilan d'eau. Comme la demande devrait être doublée d'ici 2030, on s'attend à ce que pendant une période de sécheresse (<700 mm de pluie), le réservoir ne puisse pas répondre à la demande en eau avec le risque que le réservoir se vide pendant la saison sèche. Le changement climatique pourrait avoir un effet aggravant si la fréquence et l'intensité des

sécheresses augmentent. L'interruption des prélèvements d'eau sur une longue période affectera les résidents locaux qui dépendent de cette ressource.
Les résultats de cette étude mettent en évidence l'importance de la collecte et de l'analyse des données afin de comprendre le comportement du réservoir et de son bassin versant adjacent dans un contexte hydrologique. La quantification des composantes du bilan d'eau est une tâche importante pour les Agences de l'Eau; car elle soutiendra l'élaboration de stratégies opérationnelles pour l'approvisionnement en eau et l'allocation d'eau et elle peut contribuer à la conception et à la mise en œuvre de la politique de l'eau.

Mots clef : Réservoir, Bilan de l'eau, la gestion de l'eau, Analyse du scénario, Burkina Faso

Table of Contents

Abbreviations

AEG	Regional water authority of Gourma (Agence de l'Eau du Gourma)
CN	Curve Number
DEM	Digital elevation model
DGM	National Meteorological Institute of Burkina Faso (Direction Générale de la Météorologie du Burkina)
GIS	Geographical Information System
HRU	Hydrologic response unit
INSD	National Institute of Demographical and Statistical Studies (Institute National de la Statistique et de la Démographie)
MAHPH	Ministry of Agriculture, Hydraulics and Fishery Resources (Le ministère de l'Agriculture de l'Hydraulique et des Ressources halieutiques)
MCM	Million cubic meters (10^6 m^3)
ONEA	National Office for Water and Sanitation (Office National de l'Eau et de l'Assainissement)
PAGIRE	Action Plan for Integrated Water Resources Management (Plan d'Action pour la Gestion Intégrée des Ressources en Eau)
PET	Potential evapotranspiration
95PPU	95 Percent Prediction Uncertainty
SWAT	Soil and Water Assessment Tool
V	Volume, in cubic meters unless mentioned otherwise

List of Figures

List of Tables

1 Introduction

Bakoure reservoir in Burkina Faso. Photo taken by P.J. Radsma in February, 2014

1 Introduction

Quantitative water management in semi-arid areas is of great importance. As water availability in this climate is limited, it has a direct impact on societies, livelihoods of people and land productivity. To cope with water scarcity, inhabitants in semi-arid areas found effective ways to obtain and retain water. An ancient system that is still widely used and applied is the reservoir. Reservoirs in semi-arid regions are made by constructing a dam in a sloping area to intercept surface runoff from the adjacent sloping terrain that would otherwise have flown downstream through (seasonal) rivers. A spillway in the dam allows for controlled discharge of excess water. Reservoir systems are typically located on the course of an ephemeral stream and capture water in the rainy season, to be made available during the dry season (Eilander, 2013). The reservoir's water is used for irrigation, drinking, cattle breeding, fishing and domestic purposes. Indirectly, the systems contribute to increasing income of locals, limit rural out-migration and contribute to food security (Eilander, 2013).

Burkina Faso, a sub-Saharan West African country with a semi-arid climate, has been building reservoirs for a century (Boelee *et al.,* 2009). In this French-speaking country both the dam and the reservoir in its entirety are referred to as a *barrage*. Most of the reservoirs were constructed between 1974 and 1987 during an extreme period of drought that affected West Africa (Boelee *et al.,* 2009). Also thereafter, the construction of barrages continued, and it will most likely continue in the future since there are no equally economical alternatives yet that can meet the large demand for water (United Nations Development Programme, 2015).

The availability of water in the reservoirs will decrease in the future due to various causes. Substantial climatic fluctuations in recent decades, already caused a decline in rainfall, runoff and groundwater recharge (Gunasekara *et al.,* 2014), which is likely to continue. Simultaneously there is an increase in water demand due to population growth, rising living standards and development of economic activities. Furthermore there are increasing changes in land cover and land use practices in the catchment areas of reservoirs that have an impact on the hydrology (Sally *et al.,* 2011). As a result, the reduced water availability in reservoirs will increase competition for available water among the different users, which could lead to situations of dispute and conflict (Sally *et al.,* 2011).

Faced with the problem of severe water scarcity, the government has initiated an Integrated Water Resource Management approach (In French: Plan d'Action pour la Gestion Intégrée des Ressources en Eau) in 2003, which is based on the Western European water governance structure (MAHPH, 2009). The major reforms were imposed by the national government and have to be further developed at decentralized level. Therefore, five regional water agencies have been established. One of these agencies is the Agence de l'Eau du Gourma (AEG). The AEG is responsible for the water resource management of an area of 50,000 square kilometers (larger than the Netherlands) with a population of approximately 1.7 million people in southeast Burkina Faso (AEG, 2016). It has been a water board in creation, since its establishment in January 2011 (Unité Progrès Justice, 2011), which is supported by the Dutch non-profit organization World Waternet (WWn). In July 2014, both partners signed for a Water Operator's Partnership (WOP) for a period of five years, in which WWn agreed to support

and advice the AEG to strengthen the organization and provide better, more integrated and sustainable water services to the people in their command area (World Waternet, 2016). One of the priorities of the AEG is improving knowledge regarding the surface hydrology in the Gourma region and preferably by means of a hydrologic model (AEG, 2016). Therefore the focus of this academic research lies on surface hydrology and in particular on reservoirs, since this is one of the most important water resource management techniques in Burkina Faso.

To be able to indicate and to anticipate on changing water storage in reservoirs, it is important to monitor the water storage fluctuations and to understand the causes of these fluctuations. The water storage depends on the inflow, evaporation, infiltration, water consumption and discharge and how all of these are distributed throughout the year. Because some of these components are difficult to measure over a long period and on large scale, a hydrologic computer model was used as a tool to gain insight into the distribution and uses of water over space and time.

1.1 Problem definition and aim

Despite reservoirs being used for a century in Burkina Faso, data on water balance of reservoirs and their upstream catchments is scarce - upstream catchments of reservoirs are often ungauged, which complicates the analysis of the hydrologic system - and knowledge of the importance and applicability of data is insufficient. In addition, increasing water demands are calling upon adequate statistics with regard to water availability of reservoirs. As the demand increases and climate will likely change, a stage will be reached where the required water availability in reservoirs cannot be sustained without interruption of water withdrawals.

The Agence de l'Eau du Gourma is becoming the designated governmental authority with comprehensive knowledge on water resources management in the Gourma region and forms an important bridge between the state, local authorities and other stakeholders. Data on reservoir levels and weather parameters are collected by third parties, which are then requested by the AEG. However, analysis of these data, with the aim to better understand the hydrologic system of reservoirs, their upstream catchments, and the impact of climate change and increasing water demand, is hardly done. Moreover, essential data is lacking which complicates performing a comprehensive quantitative analysis. An adequate monitoring plan and knowledge on appropriate tools for analysis are therefore a must for the AEG. In addition, the AEG has raised the desire to analyze hydrologic systems by a hydrologic computer model.

Taken into account the opposed shortcomings and the aspiration of the AEG to develop a hydrologic model, two objectives have been formulated. The main objective of this study was to determine the reservoir water balance and the secondary objective was to enhance knowledge on relevant input parameters for a hydrologic model, trend analysis of water utilization, and the impact of possible climatic and water demand changes.

1.2 Research questions

Based on the research aim the following research question and sub questions have been formulated:

Based on the reservoir water balance what is the expected, average monthly and yearly availability of water in the Tandjari reservoir in the Gourma region of Burkina Faso and what are the impacts of climate and water demand changes on these quantities?

a) Which model software is most appropriate to determine a reservoir water balance based on the requirements that it can: 1) be applied in a data scarce region, 2) deal with daily weather statistics, 3) be used by hydrologists in Burkina Faso.
b) Which model input data is required and how can it be obtained, given available data and time?
c) What is the reliability and what are the limitations of the used model?

1.3 Outline

In chapter 2 the study area and climate are described within a hydrological context. In chapter 3 the methods are explained. In chapter 4 the results are presented and explained. The uncertainty and reliability of the results are discussed in chapter 5. This is followed by the conclusion in chapter 6. Finally, recommendations are given in chapter 7.

2 Site description

Water intake tower in the Tandjari reservoir for water supply to the residents of Fada N'Gourma. Photo taken by the author on May 16, 2016

2 Site description

In this chapter the study area is described and placed in a hydrological context. Paragraph 2.1 describes the location of the study area and the reservoir characteristics and paragraph 2.2 discusses the prevailing climate.

2.1 Study area

Burkina Faso has five regional water authorities, which together are responsible for the water management in three transboundary river basins; the Niger, Volta and West Coast river basin. The Tandjari catchment is situated in the east region (region l'Est) of Burkina Faso, in the province, and similar named management area 'Gourma', and in the Niger River basin, as illustrated in figure 1.

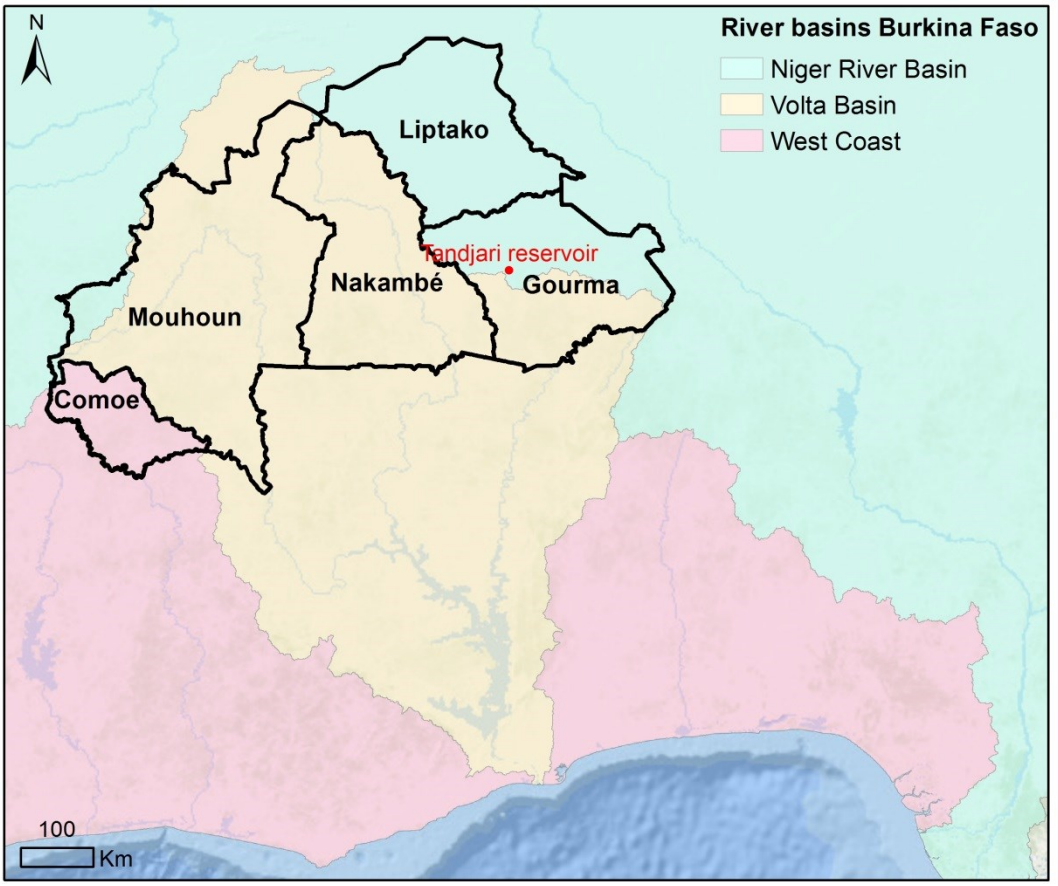

Figure 1: Hydrographic map of the river basins in Burkina Faso and the management areas of the five regional water authorities in Burkina Faso. The Tandjari reservoir is indicated in red. (Sources Esri, DeLorme, GEBCO, NOAA NGDC, AEG and other contributors)

The transboundary river basins are divided into subbasins. The reservoir is located in the Bonsoaga subbasin, as illustrated in the left map of figure 2. Discharged water from the reservoir

feeds a tributary river of the transboundary Bonsaoga River, which drains to the Niger river in the neighbouring country Nigeria. The reservoir is fed by overland runoff and seasonal rivers that discharge only during and shortly after the rainy season.

The catchment area of the reservoir is situated in the two districts Fada N'Gourma and Yamba. It is 240 km east from the capital city Ouagadougou and 20 km north from the city Fada N'Gourma and accessible via the national route N°18 Fada – Bilanga, as illustrated in the right map of figure 2.

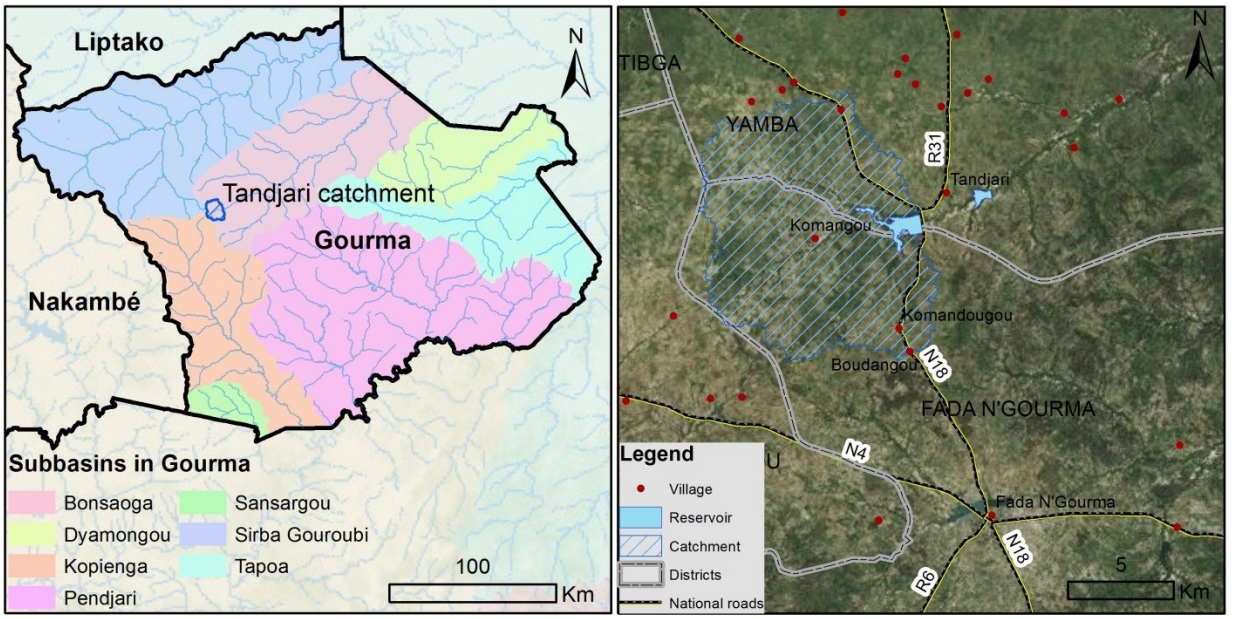

Figure 2: Left: Subbasins in the Gourma region. Right: Areal map including the location of the Tandjari reservoir (highlighted in blue) and the associated catchment (hatched) (Esri et al., 2016-2).

The Tandjari dam was initially built as a dike which served as a corridor for traffic to pass the valley. A lowered part of the dyke served as a passage for water in the rainy season. When it turned out that the dyke was also effective in retaining water it was decided to convert the dyke into a dam by raising it and constructing a spillway with on top a bridge for traffic. With the reconstruction a reservoir was created, which retains water year-round that is used for cattle breeding, cultivating crops, fishing and drinking water (O. Chanoine, personal communication, May 12, 2016). In the vicinity of the reservoir are four villages, with a total estimated population of approximately eight thousand persons (INSD, 2006).

The Tandjari reservoir is characterized by a total depth, from deepest point up to the crest level of the dam, of 8 meters. The deepest point is in proximity to the dam and the tail ends are shallow. The reservoir storage varies strongly with the season; in the rainy season the water surface can reach up to 225 hectare with a maximum depth of 6.5 meters (level up to spillway), while in the dry season it can be 76 hectare at a maximal depth of 3.9 meters according to the lowest water level record (ONEA, 2016) (SEREIN-GE SARL, 2014).

The geology in the catchment is characterized by a top layer of sandy clay and gravelly soil (<40 cm) on hard rock (schists, migmatites and undifferentiated granites), which thickness

varies much (Ministere de l'Eau Direction de l'Inventaire des Ressources Hydrauliques & Iwaco, 1993).

The vegetation in the area consists of savannah trees and shrubs. During the rainy season the area turns into a green oasis of seasonal grasses and plants. The average depth to groundwater in the wide region is estimated to be 7 to 25 meters below ground level according to an empirical based groundwater model (MacDonald & Bonsor, 2011).

Land use is dominated by pasture and agricultural land. Crops that are cultivated consist of millet, sorghum, peanuts, cassava, tomatoes, zucchini and rice (Mr. Lompo, personal communication, June 30, 2016).

2.2 Climate

Following the Köppen-Geiger climate classification, the Tandjari watershed has a typical hot semi-arid climate (BSh) with an average annual rainfall and potential evapotranspiration (obtained over the period 1900-2012) of respectively 828 mm and 1905 mm (CRU, 2016). The dryness index (F = PET/P) of 2.3 indicates that hydrologic system is subject to a regime whereby evapotranspiration is limited by water availability. Only during the rainy season, of approximately four months (June-September), the rainfall exceeds the evapotranspiration. The supply-demand framework and the Budyko curve, presented in figure 3, indicate that the fraction of the rainfall that becomes runoff (blue shaded area) is significantly smaller than the fraction that becomes actual evapotranspiration (green shaded area). It should be noted that the figure provides a reference condition for the water balance of the catchment area, however in reality this could deviate from the Budyko curve mean.

The rain season usually starts in June and ends in September. The trend of the recent years shows that rainfall is becoming more erratic and concentrated in the months July, August and September (AEG, 2016).

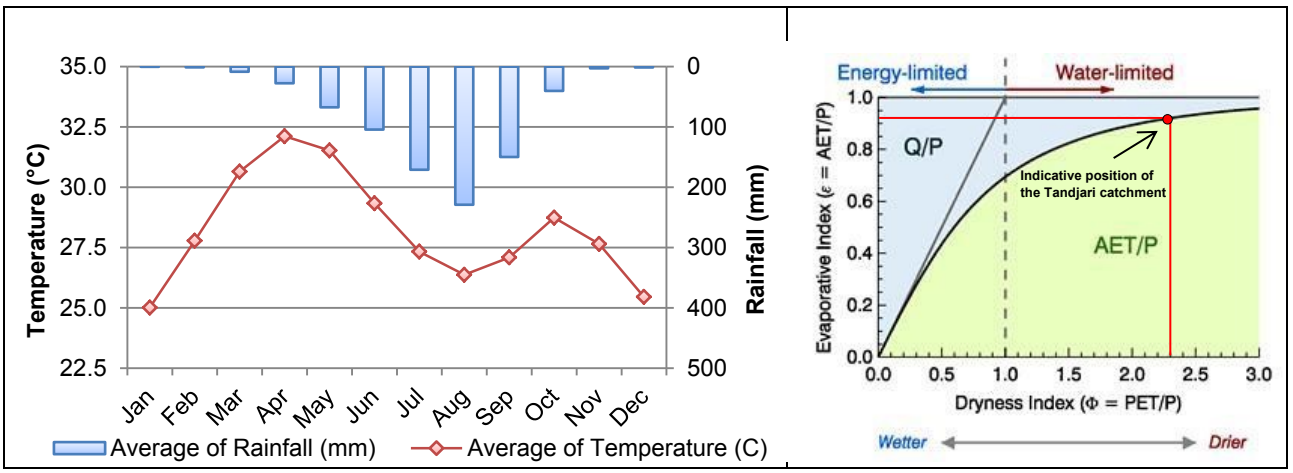

Figure 3: Left: Average monthly temperature and rainfall at the Tandjari dam (lat.12.19, lon. 0.33) *from 1900-2012. Adapted from CRU (2016). Right: Indicative positioning of the Tandjari Catchment (indicated by the red dot) on the Budyko curve (black line) and the supply demand framework. Reprinted from Description of the water-dependent asset register for the Gloucester subregion. Commonwealth of Australia (2016). The horizontal line at the top represents the water-limit,*

3 Methods

Private weather station at the Tandjari dam. Photo taken by the author on May 18, 2016

3 Methods

This chapter describes the methods used in this research. Firstly the theory behind the reservoir water balance is explained in paragraph 3.1. Secondly the applied method for the quantification of the components of the reservoir water balance is described in paragraph 3.2. Lastly the data gathering and analysis during the fieldwork in Burkina Faso are discussed in paragraph 3.3.

3.1 Reservoir water balance

A reservoir can be considered as an open water storage system wherein the surface water interacts with the atmosphere and the subsurface. The reservoir is subject to changes in climatic conditions, changes of the subsurface and the abstraction of water by humans and livestock. The components of the reservoir water balance include rainfall runoff, rainfall on the water surface, evaporation, water consumption, discharge and infiltration in the reservoir bottom (figure 4). The change in water storage is expressed by the following water balance equation:

$$\frac{dRS}{dt} = (PCP - EVAP - INF)A + RR - DISCH - CONS \quad (1)$$

where *dRS / dt* (L^3T^{-1}) is the change in reservoir storage over time, PCP (LT^{-1}) rainfall, EVAP (LT^{-1}) evaporation, INF (LT^{-1}) infiltration, A (L^2) water surface area, RR (L^3T^{-1}) rainfall runoff, DISCH (L^3T^{-1}) discharge by the spillway, and CONS water consumption. The in- and outgoing fluxes are discussed in paragraphs 3.1.1 and 3.1.2., respectively.

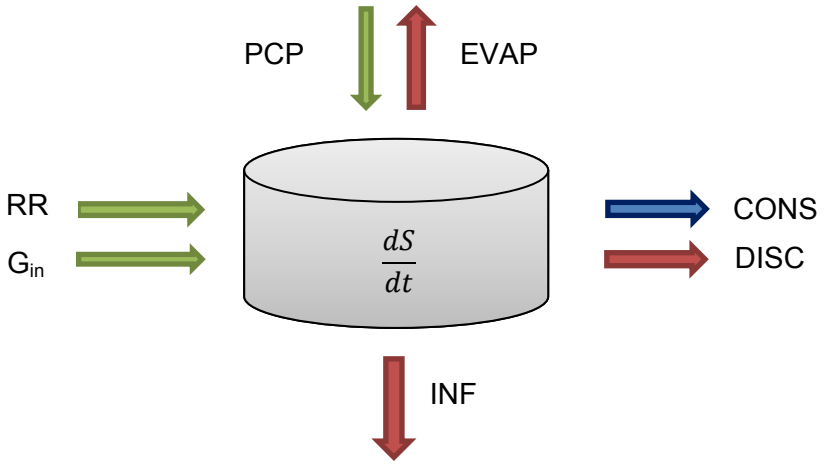

Figure 4: Schematization of the reservoir water balance

3.1.1 Incoming fluxes: rainfall and rainfall runoff

The Tandjari reservoir is rain fed. The rainfall reaches the reservoir in three ways: 1) rainfall falling directly on the reservoir, 2) runoff that is caused by rainfall on the sloping terrain in the reservoir's catchment area, and 3) groundwater inflow from the shallow aquifer to the reservoir. Overland runoff collects in three ephemeral streams that lead to the reservoir. The runoff generation in semi-arid regions follows often a typical pattern where first rains at the start of the rainy season wet up the soil that have been dried out during the dry season. These rains produce little runoff since the water is taken up mostly by the soil. Excess water flows from the catchment area to the reservoir (lowest elevation) when the soils reach field capacity. The contributing area increases with the size of the storm (Liebe *et al*., 2009).

3.1.2 Outgoing fluxes: evaporation, infiltration, discharge and water consumption

The reservoir storage decreases by evaporation, infiltration, water consumption and discharge. Evaporation and discharge vary strongly with the season. Evaporation is the rate of water transformation to vapor from the surface water in the reservoir. The flux is dependent on the potential evaporation and the surface area of the reservoir. The potential evaporation is greatest in the dry season because of high temperatures, low humidity and clear skies, whether in the rainy season the potential evaporation is reduced because clouds block the sun more often, the temperature is lower and the air more humid. The reservoir's surface area, on the other hand, is getting smaller during the dry season and reaches its maximum in the rainy season, when water is discharged from the reservoir as water levels exceed the crest level of the spillway. The outflow by the spillway is referred to as discharge.

Infiltration is the water that penetrates into the subsurface. The infiltration rate through the saturated soil at the bottom of the reservoir depends on the texture, structure and degree of heterogeneity of the soil (Hendriks, 2010).

Water that is abstracted from the reservoir by humans and cattle is considered as water consumption. Cattle use the reservoir directly for drinking and humans use the reservoir for a variety of purposes such as drinking water, irrigation, domestic use and for the production of clay bricks.

3.2 Model types for determining the reservoir water balance

A water balance could have been calculated with a spreadsheet model based on physical formulas. This type of model relies heavily on field data since spreadsheet models are not the right environment for developing comprehensive algorithms for calculating fluxes based on missing input data. Such a model allows only one component of the water balance to be unknown, since this component can be derived from the water balance formula. However, Gourma is a data scarce region making it difficult to gather sufficient data for a simple spreadsheet model.

Another possibility was using a numerical computing environment such as Matlab to develop a more advanced hydrologic model, although manually developing algorithms for various hydrologic processes is time consuming and requires experience with the programming language. Given the limited time for this study, this option was excluded.

A third option was a hydrologic model, based on build-in scripts, that allows complex hydrologic processes to be modeled. A widely used distributed hydrologic model that is praised

for its good user interface and that is well documented is the Soil and Water Assessment Tool (Arnold *et al.,* 1998). SWAT is a quasi-physical distributed continuous time model that allows a number of physical processes to be simulated in a watershed. SWAT was selected among the existing numerous hydrologic models because 1) it is open source software that runs on a Geographical Information System (GIS) interface which allows GIS specialists in Burkina Faso to use to model; 2) the model can be supplemented with built-in data that comes with the SWAT installation, which makes it useable in a study area for which limited data is available; 3) The SWAT model incorporates a rainfall-runoff method (SCS Curve Number method) that allows calculating runoff based on daily rainfall recordings, which were provided by the National Meteorological Institute of Burkina Faso (in French: Direction Générale de la Météorologie du Burkina) (DGM). 4) As additional advantage the model can be extended for analyzing sedimentation, agricultural management, stream routing and water quality, however, this study focused on the hydrologic component, and in particular on the surface runoff and reservoir water balance features.

3.3 The Soil and Water Assessment Tool model

SWAT takes the heterogeneity of the watershed into account by dividing the watershed into hydrologic response units (HRUs). The HRUs are delineated by overlapping elevation, soil and land cover data in a geographical information system (GIS). HRUs are the smallest spatial units of the model with a similar land cover, soil and slope class, based upon user-defined thresholds, whereby each unique HRU has a different effect on hydrology (Zheng *et al.,* 2009).

The hydrologic model is based on the water balance for four storage components: (1) surface, (2) soil profile, (3) shallow aquifer, and (4) deep aquifer by considering rainfall, interception, evapotranspiration, surface runoff, infiltration, percolation and subsurface runoff. Water that percolates from the soil profile is assumed to recharge the shallow aquifer. Once the water percolates to the deep aquifer it is lost from the system and cannot return.

SWAT uses, amongst others, potential evapotranspiration (PET) to calculate various water balance components. There are three methods in SWAT that can be used to calculate the PET: Hargreaves (Hardgreaves and Samani, 1985), Priestley-Taylor (Priestley and Taylor, 1972), and Penman-Monteith (Monteith, 1977; Allen 1986). For this study the Penman-Monteith method was used to calculate the PET, because this method takes most weather parameters that are available into consideration

SWAT incorporates two rainfall-runoff methods: the SCS Curve Number Method (United States Department of Agriculture and Soils Conservation Service, 1954) and the Green-Ampt Mein-Larson method (Green and Ampt, 1911; Mein and Larson, 1973). The fundamental differences between the two methods are the modelling processes and the time steps that they use. The Curve Number (CN) method is an empirical method, based on 20 years of empirical research to rainfall-runoff relationships, which takes only total daily rainfall into account. The Green-Ampt Mein-Larson method, however, is a physical method that takes the intensity and duration of sub daily rainfall into account (King *et al.,* 1999). The CN model was used for this particular research since daily rainfall statistics were actually available for the Tandjari

catchment unlike sub daily statistics. A more detailed description of the CN method is given in annex 3.

A kinematic storage routing method, which is based on slope, slope length and hydraulic conductivity, was used to calculate lateral flow in each soil layer. Lateral flow occurs when the storage in any layer exceeds field capacity (Neitsch et al., 2009). Lateral flow and surface runoff of all HRUs are summed and then routed through the stream network to the reservoir by using the variable storage routing method, which is based on the kinematic wave model. More information about the kinematic wave model can be found in Dingman (2015).

Weather data is one of the most essential inputs of the model. SWAT requires daily data for rainfall and minimum and maximum temperature. The built-in weather generator program WXGEN (Sharpley and Williams, 1990) in SWAT allows simulating missing weather data.

Reservoir parameters in SWAT are used to calculate outgoing reservoir fluxes consisting of (1) evaporation, (2) infiltration, (3) water consumption and (4) discharge. Evaporation and infiltration are fluxes to respectively the atmosphere and the subsurface and can be considered as non-productive reservoir losses. Evaporated reservoir water is practically irrecoverable where infiltrated water may contribute to aquifer recharge and can thus be recovered from the surficial aquifer system. (1) Reservoir evaporation is derived from the potential evaporation using a conversion factor i.e. evaporation coefficient. (2) The monthly reservoir infiltration is based on the hydraulic conductivity of the reservoir bottom. The method used to obtain a value for this parameter is described in paragraph 3.2.2.1. (3) Water consumption is considered as removed water from the reservoir for use outside the watershed. Monthly values of this parameter are obtained from literature, field observations and interviews, which are described in detail in paragraph 3.2.2.2. (4) Reservoir discharge depends on the reservoir operation. The Tanjari reservoir is an uncontrolled reservoir that releases water whenever the reservoir level exceeds the spillway level. To simulate an uncontrolled reservoir the option ‘simulated target release rate’ is selected in SWAT. The entire year is indicated as a “flood season” and all 12 monthly target volumes are set to the reservoir volume at spillway level (4.750.000 m³). The number of days to reach target storage from current reservoir storage is set to 1. SWAT is not able to abstract the reservoir bathymetry from the digital elevation raster; hence this input has to be entered explicitly. The method that is used by SWAT to calculate the reservoir storage is further explained in chapter 3.2.4.

3.3.1 Model setup

The model setup was done using the ArcView GIS interface for SWAT (Di Luzio *et al*., 2001). In the first step, delineation of the watershed, i.e. determining the size of the water catchment area in the terrain of interest and the division of subbasins were done based on the digital elevation map. Also the reservoir was included in the stream network. The parameterization of the stream reaches, stream length, area, slope, and elevation distribution were done automatically by the interface.

In the next step SWAT divides the watershed into hydrologic response units (HRUs) based on the soil, land cover and elevation data.

In the following step weather data was uploaded, which also determined the type of rainfall runoff model that was used. Daily rainfall was added which necessitated using the SCS

Curve Number method. Additionally maximum and minimum temperatures and average daily wind speed, relative humidity and solar radiation were used as weather input data.

In the second last step reservoir parameters were added. SWAT does not have the feature to enter an area-volume equation but SWAT creates an equation itself, based on the interpolation between two known (blue marked) points from the bathymetry data as presented in figure 5. It means a rather big compromise on the resolution of the data. A more detailed description of the formula can be found in Annex 2. The following exponential equation was obtained by SWAT:

$$SA = 0.0007323 * V^{0.8218860} \quad (2)$$

Where SA is the surface area of the reservoir in hectares and V is reservoir storage in cubic meters. The green graph in figure 5 shows the area-volume relation obtained by a bathymetric survey in March 2014 and the blue graph the area-volume relation by SWAT.

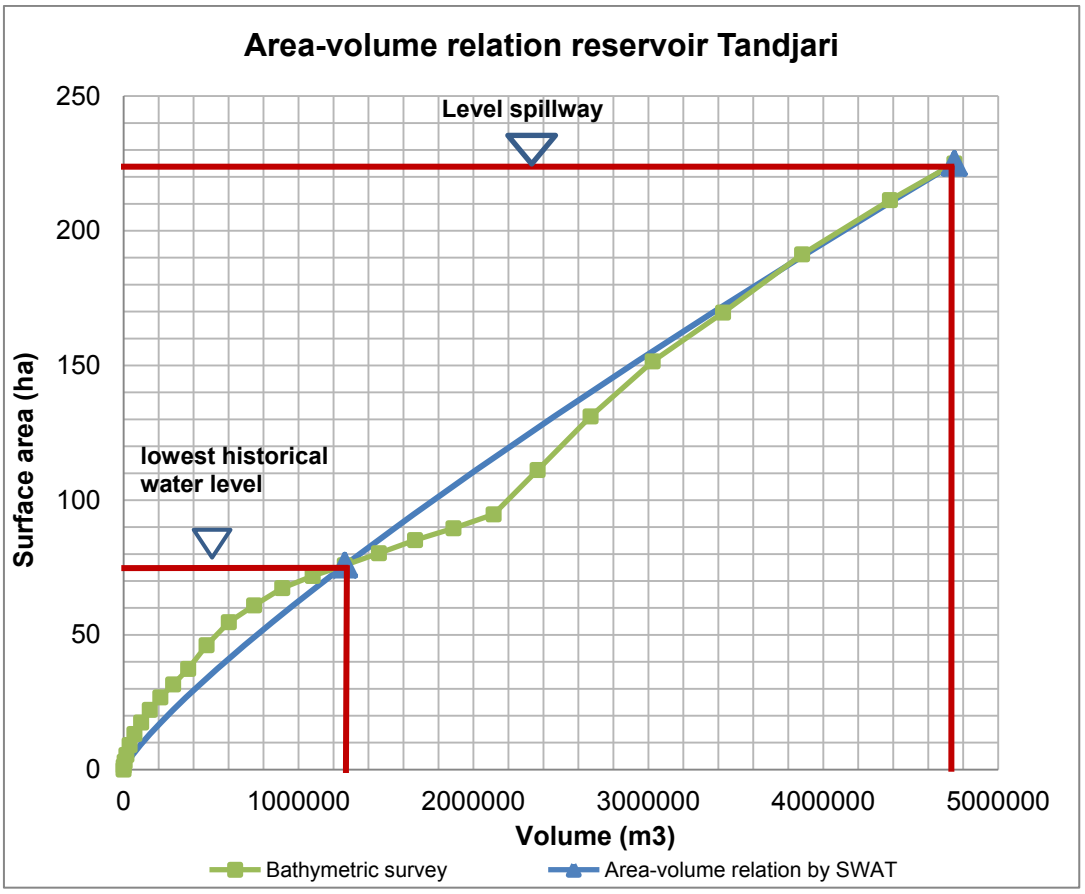

Figure 5: Actual area-volume relation by SWAT compared to the observed area-volume relation obtained from the Bathymetric survey in March 2014

At this stage all the available input data was fed into the model that was ready for initial simulating. The entire simulation period is from 2010 to 2016. The first two years were used as a warm-up period in order to mitigate the initial conditions, and were excluded from the analysis.

SWAT calculates the reservoir evaporation from the potential evapotranspiration by using a reservoir evaporation coefficient.

3.4 Acquisition of reservoir parameters by fieldwork

The following paragraphs describe how fieldwork has contributed to find an affective value for the hydraulic conductivity of the reservoir bottom and to obtain monthly values of water consumption. In paragraph 3.3.1 the infiltration experiment is described and in paragraph 3.2.2.2 is explained how the consumption data was obtained. The fieldwork was conducted in the period from May till July in 2016.

3.4.1 Hydraulic conductivity of the reservoir bottom

Infiltration is sometimes disregarded in reservoir water balance calculations because it is considered difficult to estimate or measure (Andreini, 2016). However, given the bathymetry of the reservoir; shallow depth and large surface area, there might be significant infiltration. The hydraulic conductivity of the reservoir bottom cannot simply be based on the saturated hydraulic conductivity of the surrounding soil(s) because the texture of the reservoir bottom will most likely differ due to sediment and organic matter from ephemeral streams that have settled on the bottom. For this reason it is decided to conduct infiltration measurements in order to obtain an effective saturated hydraulic conductivity of the reservoir bottom which is used by SWAT to calculate the monthly reservoir filtration.

The reservoir's infiltration rate depends on the texture, the structure and the heterogeneity of the soil. A heterogeneous soil can be considered as a succession of single, homogeneous soil layers. In a heterogeneous soil, assumed that there are no cracks, the infiltration capacity equals the weighted average infiltration rate of the separate layers (Eijkelkamp, 2015). With five obtained infiltration rates on different locations of the reservoir bottom, the average nearly saturated infiltration capacity K_{sat} was calculated. With this parameter the total volume of water that infiltrated in the reservoir bottom in time was determined.

The infiltration rates at the five locations along the reservoir shore were measured with a double ring infiltrometer, made by a local whitesmith in Fada N'Gourma, and a Mariotte bottle, which allowed the water level in the infiltrometer to be constant and to keep track of the infiltrated water. The double ring infiltrometer consists of two open rings - one with a larger diameter than the other - that were penetrated into the soil. The inner ring is used for the infiltration measurement and the purpose of the outer ring is to have the infiltrating water act as a buffer zone against infiltrating water straining away sideways from the inner ring (Eijkelkamp, 2015).

Both rings were filled with water to the same level and a soft plastic tube was placed between the Mariotte bottle water outlet and the inner infiltrometer ring, as presented in figure 6. The Mariotte bottle was filled with water that stayed in contact with the water in the inner ring. A cork with an air inlet pipe closed the bottle. At both the bottom level of the air inlet pipe and at the free water surface in the inner ring, the water pressure was equal to the atmospheric pressure i.e. both the Mariotte bottle and the water level in the inner ring were communicating vessels. When water infiltrated in the soil, the water level in the inner ring dropped slightly, this

caused water to flow from the Mariotte bottle into the inner ring until the water levels were equal again.

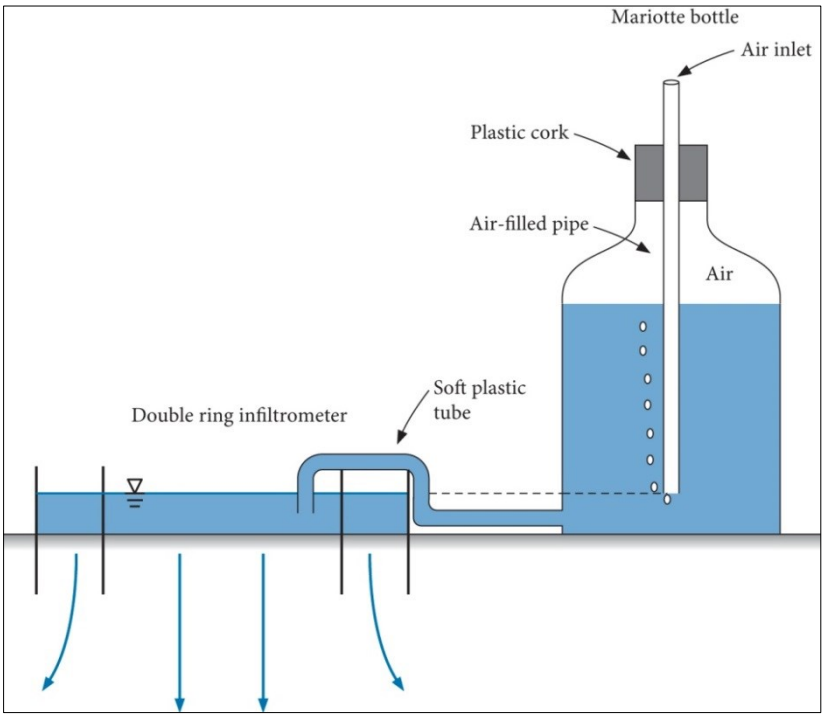

Figure 6: The double-ring infiltrometer and the Mariotte bottle. Reprinted from Hendriks, 2010.

During the experiment the time and the water level in the Mariotte bottle were recorded. Dividing the change in water level by the passed time gave the discharge rate of the Mariotte bottle in mm hour^{-1}. Multiplying this discharge rate by the ratio between the surface area of the Mariotte bottle and surface area the inner infiltroring yielded the rate at which water had infiltrated and evaporated from the inner ring in mm hour^{-1}. To obtain an accurate nearly saturated cumulative infiltration rate, the water level drop in the Mariotte bottle needs to be compensated by the water that evaporated during the experiment. The local evaporation was measured with a Class A evaporation pan. The pan was filled with approximately 5 cm of water after being leveled. The difference in height (mm) divided by the time interval (hours) resulted in the pan evaporation in mm hour^{-1}. The pan evaporation will generally be higher than the open-water evaporation; this is due to the extra energy a pan receives through its sides and bottom (Jones, 1991). This effect is negligible for the inner ring of the infiltrometer, since this ring is surrounded by water from the outer ring. To compensate for this error a multiplication factor of 0.8 was used (Linacre & Geerts, 1997).

With the obtained nearly cumulative infiltration rate, the nearly saturated hydraulic conductivity K_{sat} was calculated by using the Philips equation. This equation describes the cumulative infiltration f in (mm), which is depending on time t (h), the sorptivity S (mm h$^{-1/2}$), and the saturated hydraulic conductivity K_{sat} (mm h^{-1}):

$$f = \frac{1}{2} S t^{-0,5} + K_{sat} \quad (3)$$

For the S holds that the slope of the graph is 1/2 S. Given this, S was calculated by computing the formula: S= 2*11,092=22,184 mm $s^{-0,5}$.

The average of all the calculated K_{sat}- values gave an effective value for the hydraulic conductivity of the reservoir bottom.

3.4.2 Monthly water consumption parameters

Predominantly the reservoir's water is used as drinking water supply to the residents in Fada N'Gourma. Water is withdrawn from the reservoir by a water intake tower and transported under pressure, over a distance of approximately 20 kilometers, to the water treatment plant in Fada N'Gourma. Statistics of the monthly water withdrawal are made available by the ONEA. Locally, the reservoir supplies water for; irrigation in agricultural, domestic use (for example washing and cooking), and for both human consumption and livestock. These additional monthly water withdrawals were estimated based on field observations, interviews with local residents, and by statistical data that were provided by the Provincial Department of Agriculture, the Provincial Department of Animal Resources, and the Central Office of the Census. Interviews clarified which villages are dependent on the reservoir for their water needs. Daily water quantities that were abstracted from the reservoir by local residents were estimated based on field observations. For livestock the daily water demand figures were taken from the Veterinary Manual (Ministère de la coopération et du développement, 1988). The population and livestock numbers were obtained from respectively the Central Office of the census and the Provincial Department of Animal Resources. Pump capacities of irrigation pumps were verified by field observations and statistics with regard to irrigators provided by the Provincial Department of Agriculture.

3.5 Model parameterization

SWAT input parameter values were obtained from an online database, governmental and semi-governmental organizations, field measurements, literature, and interviews.

To determine the HRUs, SWAT needs input data on elevation levels, soils and land cover.

I. A Digital elevation raster, with a resolution of 30x30 meters (1 arc-second) was obtained from the NASA Shuttle Radar Topography Mission (SRTM) and provided by the U.S. Geological Survey's (USGS) Long Term Archive (LTA) at the National Center for Earth Resource Observations and Science (EROS) in Sioux Falls (2015). Retrieved from https://lta.cr.usgs.gov/SRTM1Arc.
II. A soil map was developed and provided by the AEG (2016). A soil data base with soil properties including amongst others; a minimum of two soil layers, texture (%age clay/silt/sand/rock/organic matter), saturated hydraulic conductivity, available water capacity (pF2,5/pF3,0/pF4,2) and rooting depth were provided by Wellens (2016). Soil

properties in the database are derived from soils in the Kou Watershed in West Burkina Faso.

III. Land cover data was provided by the AEG (2016). The parameterization of the land cover classes including SCS Runoff Curve Numbers, leaf area index, maximum stomatal conductance, maximum root depth, and optimal and minimum temperature for plant growth were based on the available SWAT land cover classes.

The hydrologic cycle that is simulated by SWAT is climate driven and requires moisture and energy input, such as daily rainfall, maximum/minimum air temperature, wind speed, relative humidity and solar radiation that control the water balance.

IV. Daily weather statistics including rainfall, maximum/minimum temperatures, average daily wind speed and relative humidity were provided by the National Meteorological Institute of Burkina Faso (in French: Direction Générale de la Météorologie (DGM) du Burkina) and obtained from a private weather station. The data originates from a DGM weather station at the airport of Fada N'Gourma (12°02'44.8"N 0°21'52.2"E) at 15 km distance of the Tandjari reservoir and from a self-installed weather station at the Tandjari dam (2°11'17.6"N 0°19'57.9"E). The DGM data covers the years from 1984 to 2016 and the private weather station at the Tandjari dam has collected data from May 2016 to December 2016. Daily averaged solar radiation data was obtained from the NASA Surface Meteorology and Solar Energy database (Stackhouse, 2017). Gaps in weather parameter data were supplemented by generated data using the built-in weather generator program WXGEN (Sharpley and Williams, 1990).

Other data demanded by SWAT are parameters for reservoir characteristics, reservoir management and monthly water consumption.

I. Reservoir characteristics consist of (1) date of construction, (2) storage capacity, (3) hydraulic conductivity of the reservoir bottom, and (4) a reservoir evaporation coefficient. (1) Structural details with regard to the construction of dam, including year of construction, dimensions and altitudes were obtained from the report 'Suivi-controle des travaux de rehabilitation du barrage de Tandjari, province du Gourma, region de l'Est' (ONEA, 2015). (2) The storage capacity of the reservoir was obtained from bathymetry data that was presented in the report: Realisation des travaux d'installation d'echelles limnimetriques et de leves bathymetriques et topographiques sur les barrages d'itengue, de salbisgo, de tandjari et de yakouta (SEREIN-GE SARL, 2014). The bathymetric survey of the Tandjari reservoir was carried out in March 2014 by SEREIN-GE SARL that used advanced equipment including a RTK GPS (Real Time Kinematic Global Positioning System) system to obtain coordinates and altitudes along the waterline and a boat equipped with an ultra-sounder and GPS to register water depths (figure 7). The equipment could measure depth with 0,2% accuracy and a spatial resolution of 1 cm.

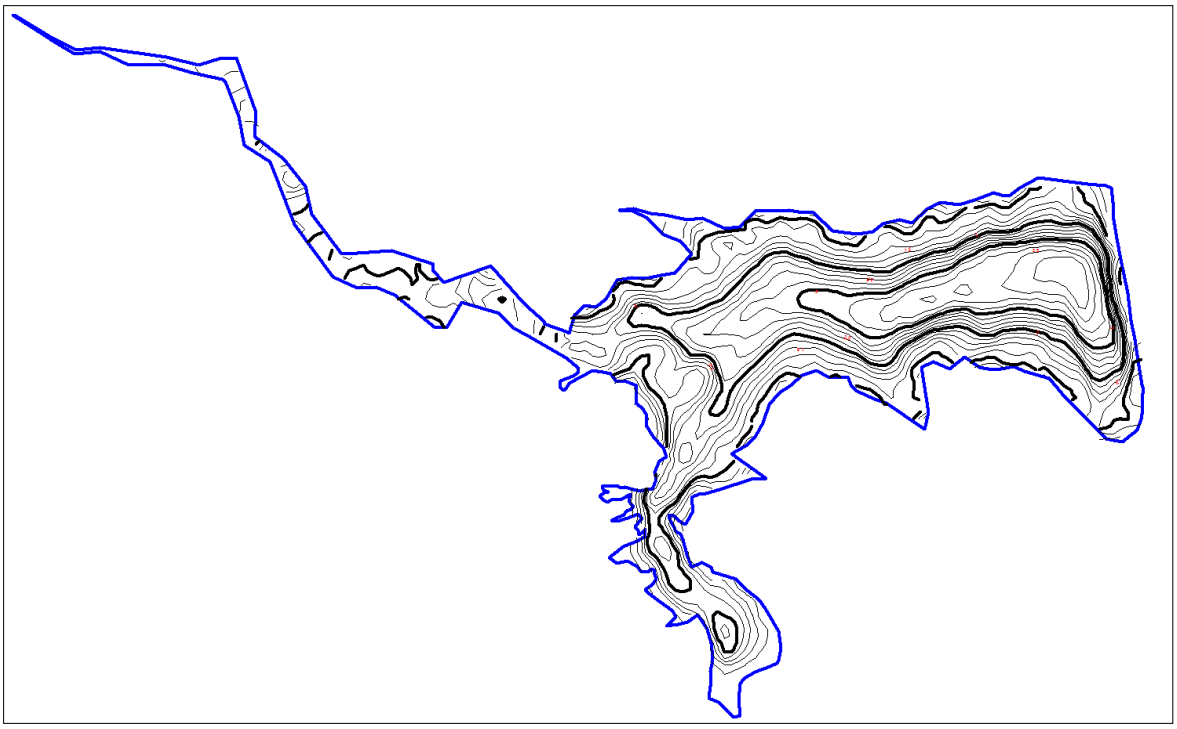

Figure 7: Bathymetric chart of the Tandjari reservoir. Reprinted from SEREIN-GE SARL, 2014.

(3) Hydraulic conductivity of the reservoir bottom is obtained by field measurements as described in chapter 3.2.2.1. (4) Reservoir evaporation, also referred to as open water evaporation (ETo), is calculated in SWAT as a factor of the potential evapotranspiration (PET) by a reservoir evaporation coefficient (EVRSV). EVRSV is set to 1 in the default simulation, meaning that reservoir evaporation is initially assumed as being equal to the PET. However, ETo might be lower than PET, in sub humid/arid regions, according Rosenberg et al. (1983), which is why this parameter will later on be used in the calibration procedure.

3.6 Sensitivity analysis

Sensitivity analyses in SWAT-CUP were conducted to evaluate the effect of changes in various model parameters on the simulated reservoir storage, and to identify parameters, which had no significant effect on the output, so that these redundant parameters could be left out of the model calibration. SWAT contains hundreds of parameters making it unfeasible to include all parameters in the sensitivity procedure; therefore a pre-selection of the most relevant parameters was needed, which was based on Schuol *et al.* (2006) and Schuol *et al.* (2008).

Two sensitivity analysis methods were used: 1) A one-parameter-at-a-time sensitivity analysis and 2) a global sensitivity analysis. In the first method, changing one parameter, while other parameters remained constant assessed the effect on the model outcomes. The downside of this method is that it does not take into account the consideration that the sensitivity of one parameter may also depend on the value of other parameters (Abbaspour, 2015). The global

sensitivity analysis on the other hand, assessed the sensitivity of a parameter relative to simultaneous changes of other parameters. A multiple regression system, which regresses the Latin hypercube generated parameters against the objective (KGE) function values, was used to estimate the global sensitivities (Abbaspour, 2015). A t-test was then used to identify the relative significance of each parameter. In this analysis the larger the absolute value of the t-test, and the smaller the p-value, the more sensitive the parameter (Abbaspour, 2015). Based on the sensitivity analysis some parameters that were not sensitive were left out, while other important parameters, that directly influence the reservoir balance, were added to the calibration procedure that is explained in the next section.

3.7 Calibration and validation

The calibration and uncertainty analysis were done automatically using the program SUFI-2. This program is linked to SWAT in the calibration package SWAT Calibration and Uncertainty Programs (SWAT-CUP) developed by Eawag (2009) (Abbaspour, 2015). SUFI-2 allows calibrating a large number of parameters and iterations simultaneously. In SUFI-2, uncertainty in parameters accounts for all sources of uncertainties, such as uncertainties in driving variables (e.g., rainfall), conceptual model parameters, and measured data (Schuol *et al.* 2008). The degree to which all uncertainties are accounted for is quantified by two measures, referred to as the P-factor and the R-factor. The P-factor is the percentage of measured data that falls within the 95% prediction uncertainty, hereafter called the 95PPU. The 95PPU is calculated at the 2.5% and 97.5% levels of the cumulative distribution of an output variable - in this study the reservoir storage - using Latin hypercube sampling (Schuol *et al.* 2008). As all sources of uncertainties are accounted for in this measurement, the degree to which the 95PPU does not include the measured data indicates the prediction error. Theoretically, the value for the P-factor ranges between 0 and 100%, where an ideal value of 1 indicates that 100% of the measured data was within the 95PPU band, hence accounting for all the correct processes. The R-factor, on the other hand, measures the quality of the calibration by indicating the thickness of the 95PPU band. The value of the R-factor ranges between 0 and infinity and should ideally be near zero. The combination of the P-factor and the R-factor indicate the goodness of fit and the strength of the model calibration and uncertainty assessment (Arnold et al., 2012).

Parameters with a large effect on the reservoir storage were selected based on a sensitivity analysis that was conducted in SUFI-2. A selection of 13 parameters, as presented in table 1, was chosen for calibration and validation of the model. As increasing parameter uncertainty also increases the output uncertainty, the calibration procedure SUFI-2 starts by assuming a large parameter uncertainty, so that the measured data initially falls within the 95PPU, then decreasing this uncertainty in steps while monitoring the P-factor and the R-factor. Parameters are updated in such a way that the new parameter value ranges, as indicated by table 1, are always smaller than the previous ranges, and centered around the best simulation (Schuol, Abbaspour, Srinivasan, & Yang, 2008). In total 500 simulations were carried out during the calibration procedure and the simulation with the best parameter set was selected based on the model performance indicators which are in the next alinea.

Table 1: Upper and lower boundary values for parameters that were used for calibration

		Initial range		Final range	
Parameter name	**Definition**	**min**	**max**	**min**	**max**
r_CN2.mgt	Curve number factor applied to all soil types (-)	-0.4	0.4	-0.4	-0.2
r_SOL_AWC.sol	Soil available water storage capacity (mm water/mm soil)	-0.4	0.4	-0.3	-0.2
r_SOL_K.sol	Soil hydraulic conductivity (mm/hr)	-0.5	0.5	-0.4	-0.2
v_RES_K.res	Hydraulic conductivity of the reservoir bottom (mm/hr)	0.06	1	0.06	0.21
v_EVRSV.res	reservoir evaporation coefficient	0.8	0.9	0.8	0.9
v_ALPHA_BF.gw	Baseflow alpha factor (days)	0	0.4	0.01	0.4
v_GW_DELAY.gw	Groundwater delay time (days)	0	400	100	300
v_REVAPMN.gw	Threshold depth of water in the shallow aquifer to the root zone (mm)	0	40	30	40
v_GW_REVAP.gw	Groundwater 'revap' coefficient (-)	0.02	0.2	0.1	0.2
V_RCHRG_DP.gw	Deep aquifer percolation factor (-)	0	0.7	0.1	0.3
V_ESCO.hru	Soil evaporation compensation factor (-)	0.01	1	0.01	0.2
MSK_CO1	Calibration coefficient that controls impact of the storage time constant for normal flow (1)	0	10	0	2
NSK_CO2	Calibration coefficient that controls impact of the storage time constant for low flow (-)	0	10	8	9

v_ : means the default parameter is replaced by a given value, and r_ means the existing parameters value is multiplied by (1 + a given value)

The parameters mentioned in the table above are defined as follows:

- SCS Runoff curve number (CN2) is a function of the soil's permeability, land cover and antecedent soil water conditions. The larger the CN the greater the runoff.
- Available water capacity (AWC) is the difference between the field capacity of the soil and the permanent wilting point. It is defined per soil layer per soil type and determines, to a large extent, the water holding capacity of the soil (mm water/mm soil).
- The Saturated hydraulic conductivity (SOL_K) is a measure of the ease of water movement through the soil and is defined per soil type (mm/hr).
- The groundwater revap coefficient (GW_REVAP) influences the process of water being evaporated from the capillary fringe in dry periods.
- The threshold depth of water in the shallow aquifer for 'revap' or percolation to the deep aquifer to occur (REVAPMN).
- The baseflow recession parameter (ALPHA_BF) is an index of the groundwater flow response to changes in recharge (Smedema *et al.,* 1983) (1/days).
- The lag between the time that water exits the soil profile and enters the shallow aquifer can be controlled by the groundwater delay time (GW_DELAY) (days).
- The fraction of percolation from the root zone which recharges deep aquifer is controlled by the deep aquifer percolation factor (RCHRG_DP)

- The reservoir evaporation coefficient EVRSV controls the amount of reservoir evaporation relative to potential evapotranspiration (PET). Reservoir evaporation might differ from PET because of other humidity and temperature conditions over water bodies.
- The hydraulic conductivity of the reservoir bottom (RES_K) determines the amount of infiltration in the reservoir bottom (mm/hr).
- The soil evaporation compensation factor (ESCO) controls the distribution that is used to meet the soil evaporative demand. The lower the value of ESCO, the more evaporative demand can be extracted from lower levels.
- MSK_CO1 and MSK CO2 are coefficients that control the impact of the storage time constant for low flow used in the Muskingum routing method.

Further correspondence between observations and the final best simulation were interpreted by the Kling-Gupta efficiency (KGE) coefficient (Gupta, 2009), the Coefficient of Determination (R^2) (Cox & Snell, 1989; Magee, 1990), and the % Bias (PBIAS). The goodness-of-fit, between the observed reservoir storage and the best calibrated simulation, was measured by the KGE and R^2, while the PBIAS determined to which degree the simulated values overestimated or underestimated the observed values. The optimal KGE values can range from negative infinity to 1, where 1 is a perfect match of simulated an observed data. The R^2 values are between 0 and 1, with 1 indicating that the model perfectly represents the observed data. The ideal % error has a value of 0.0; where positive values indicate an underestimation and negative values an overestimation of the observed reservoir storage. The formulas for the R^2, KGE and PBIAS are respectively:

$$R^2 = \frac{\left[\sum_i (Q_{m,i} - \bar{Q}_m)(Q_{s,i} - \bar{Q}_s)\right]^2}{\left[\sum_i (Q_{m,i} - \bar{Q}_m)^2 \sum_i (Q_{s,i} - \bar{Q}_s)\right]^2} \quad (4)$$

Where Q is a variable (e.g., reservoir storage), m and s stand for the measured and simulated data, i is the i^{th} measured or simulated data.

$$KGE = 1 - \sqrt{(r-1)^2 + (\alpha - 1)^2 + (\beta - 1)^2} \quad (5)$$

Where $\alpha = \frac{\sigma_s}{\sigma_m}$, $\beta = \frac{\mu_s}{\mu_m}$, r is the linear regression coefficient between the simulated and observed variable, μ_s and μ_m are means of simulated and observed data, and σ_s and σ_m are the standard deviation of simulated and observed data

$$PBIAS = \frac{\sum_{i=1}^{n} (observed\ streamflow, i\ - simulated\ streamflow, i)}{\sum_{i=1}^{n} observed\ streamflow\ , i} * 100 \quad (6)$$

The observed data used for the calibration procedure consists of reservoir storage volumes, which are based on water level measurements of the Tandjari reservoir. The ONEA has provided water level measurements of the Tandjari reservoir from the period of February 2012 to February 2015. The water level over this period was monthly registered by a visual reading from a water level gauge. The water level was then translated to storage values by using the water level-volume relation which was obtained from bathymetry data (SEREIN-GE SARL, 2014). From May 24, 2016 the water level measurements were resumed by a, for this study installed, water level data logger that had a record interval of 30 minutes (figure 8). Each 30 minutes the, so called, diver measured the water level and saved it to its internal memory. At regular times the diver was taken out of the reservoir and the data was transferred to a laptop. The observed data was both used for calibration and validation by dividing it in two data sets: one for calibration and another for validation. For the calibration procedure weather data from the DGM weather station (see chapter 3.2.3) and observed data obtained from water level records of ONEA were used, covering the period from February 2012 – February 2014. Validation was done with weather data obtained from the private weather station (see chapter 3.2.3) and observed data obtained from data logger records covering the period of May 2016 to December 2016.

Figure 8: Installation of a diver. Photos taken on August 12, 2016 by F. van Broekhoven

3.8 Climate and water demand scenario simulations

Climate and water demand scenario simulations were performed, by changing meteorological and water consumption input parameters of the SWAT model, with the objective to examine the effect of climate change and population growth on the water availability of the Tandjari reservoir.

The Intergovernmental Panel on Climate Change clearly stated in their Fifth Assessment Report (AR5), that increase in anthropogenic greenhouse gases emissions (carbon dioxide, methane, nitrous oxide) will result in global climate change. Global temperatures will rise, precipitation patterns and quantities will likely change, and the frequency and intensity of anomalies such as droughts and floods are expected to increase. African countries in particular are vulnerable to climate change due to a combination of naturally high levels of climate variability, high reliance on climate sensitive activities such as rain fed agriculture, and limited economic and institutional capacity to cope with, and adapt to, climate variability (Roudier, Sultan, Quirion, & Berg, 2011). The large scale drought in West Africa of the 1970s and 1980s, due to severe anomalies with much lower rainfall than preceding decades, had big impact on local populations (Dai et al., 2004). Burkina Faso responded to the drought by constructing many reservoirs in order to become more resilient to climatic variability (Boelee *et al.,* 2009). But this measure was not sufficient. Increasing water demand is putting more pressure on the limited surface water resources. The water demand is increasing, due to the rapidly growing population; approximately 2.54 % growth is expected between 2000 and 2050, which is the sixth-fastest rate in the world (United Nations Department of Economic and Social Affairs, 2004). Yang *et al.,* (2003) estimated that by 2030 Burkina Faso will experience water scarcity, which is defined as less available water than 1500 m^3 $capita^{-1}$ $year^{-1}$.

The large-scale drought of the 1970s and 1980s was also reflected by the low annual rainfall recordings (1984 -2016) in Fada N'Gourma (DGM, 2016). During the years from 1984 to 1987 the annual rainfall was less than 600mm. The lowest annual rainfall of 523mm was recorded in 1990 followed by 558 mm in 1986. Assuming a worst case, the scenario analysis should be based on the worst historical drought including the worsening effects of climatic and water demand changes. "Downscaled climate model projections for 2000-2050 agree on temperature increases ranging from 1 – 1.5 ºC to 3-3.5 ºC across Burkina Faso. Climate model projections for mean annual precipitation do not reflect a clear consensus, although evidence exists for the likelihood of more erratic and intense rainfall" says Snorek *et al.,* (2014).

Based on a literature analysis by Roudier et al. (2011) on climate scenarios used in various studies within Burkina Faso, West Africa and Africa in general, the climate change changes applied in this scenario analysis are rainfall changes of -5% and a temperature increase of + 1 ºC by 2030. The weather generator model WXGEN (Sharpley and Williams, 1990) was used to generate climatic data from 2027 to 2037. Historical weather data from 1984 till 2017 was used as input in order for the WXGEN to generate the future climatic data.

Predictions for changing water demand are based on growth numbers for population, livestock, and agriculture that are used by respectively the Central Office of the Census, the Provincial Department of Animal Resources, and the Provincial Department of Agriculture. These statistical data were collected during the fieldwork period in Burkina Faso. Based on the future demand analysis it was estimated that the total water consumption from the reservoir will

be doubled by 2030. Detailed results on the demand change analysis are presented in chapter 4.1.

In total three scenarios were simulated which were applied to the baseline simulation. The baseline simulation reflects conditions based on the 2016 water demand and historical climate statistics including a drought period similar to the one in 1980s. The demand scenario (D) assumes doubled reservoir water consumption and baseline weather statics. The climate scenario (CC) assumes a temperature increase (+1 ºC) and precipitation decrease (-5%), and no change in water consumption compared to the baseline simulation. The combined scenario (DCC) assumes both; climate and demand changes (table 2) compared to the baseline simulation.

Table 2: Scenarios used for reservoir balance simulations from 2027 to 2037

Scenarios	Increase or decrease from the baseline simulation		
	Rainfall (%)	Temperature (˚C)	Water consumption (%)
D	0	0	+100
CC	-5	+1	0
DCC	-5	+1	+100

4 Results

A farmer prepares for irrigation of crops. Photos taken by the Author on June 1, 2016

4 Results

This chapter presents and discusses the results of this hydrologic research. The first paragraph describes the collected and processed data that was used as input for the distributed hydrologic model. The second paragraph discusses the results of the observed reservoir storage. The third paragraph explains the results of the sensitivity analysis. The fourth paragraph presents the calibration and validation results of the model. And the final paragraph shows the reservoir water balance results from the best simulation.

4.1 Input data for the hydrologic model

In this paragraph the input data for the model consisting of HRUs, weather data, reservoir characteristics, and water consumption data, are described.

4.1.1 Land cover, vegetation, soil, and slope classification

The watershed area and the stream network were derived from the DEM (figure 9) using the watershed delineator in SWAT. This resulted in a catchment area of 104 square kilometers with 29 sub basins, which were further subdivided into 133 HRU's.

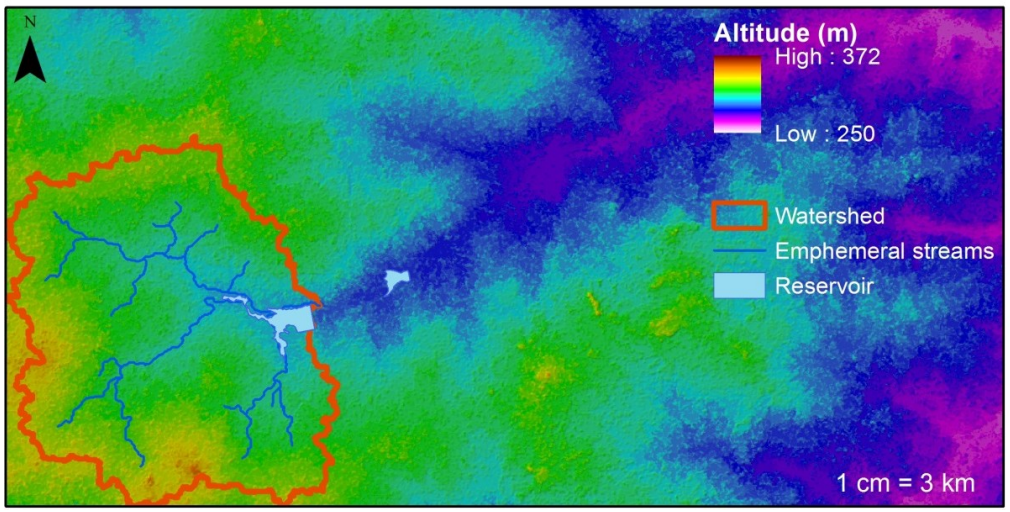

Figure 9: DEM of the Tandjari watershed based on data by NASA et al (2015). (ESRI et al., 2016-2)

The HRUs were based on soil, land cover, and slope. Pastures and savannah dominate the land cover, as illustrated in figure 11. The majority of the soil is represented by sandy gravel on a layer containing ironstone, as illustrated by figure 10. In French the soil is classified as *"Sols peu évolués d'érosion gravillonnaires sur cuirasse ferrugineuse"*. The available water capacity and the soil fertility are low (AEG, 2016). Ironstone, with a typical reddish color, is sometimes visible at the surface. Additionally ferruginous tropical soil with translocated, or concretion of, iron/clay on a sandy-clayey layer can be found in the northern part of the catchment. The topsoil and the subsoil have respectively a sandy and clayey-sandy (from 40 to 50 cm) texture. The soil fertility is low (AEG, 2016). In French the soil is referred to as *"Sols ferrugineux tropicaux lessivés ou*

appauvris à taches et à concrétions sur les matériaux argilo-sableux". The term 'lessivé' is used by French pedologists to refer to migration of iron or clay as distinguished from leaching of bases or silica. The term 'appauvri' refers to clay that appears to have been lost from the A (surface) horizon (Forbes, 1973). The two soils on the map in figure 10 are linked to the corresponding soils in the data base that was provided by Wellens (2016). The series of soil parameters obtained from the database were imported in the SWAT data base. In table 3 the sandy gravel and ferruginous tropical soil are referred to as respectively PEEL and FLTC. The hydrologic group is represented by a letter from A to D and characterizes the permeability of the soil. It has therefore an important impact on the runoff and infiltration components of the water balance. The sandy gravel belongs to group A, 'well drained-soils', which is reflected by the high saturated hydraulic conductivity (SOL_K) of 38.3 mm h^{-1} - nota bene, the overall infiltration rate depends on the layer with the lowest, saturated hydraulic conductivity. The ferruginous tropical soil belongs to group D, 'poorly drained soils', which is reflected by the low SOL_K of 2.8 mm h^{-1}. Due to the low k value, the soil has a significant runoff potential. The available water capacity (SOL_AWC) of sandy gravel soil is medium where the ferruginous tropical soil has a low available water capacity. More information about the soil parameters can be found in Lang *et al.* (2011).

The majority of the slopes in the catchment area have a gradient of 2.49% to 5.6% as can be seen from figure 12 and the HRU distribution in table 4.

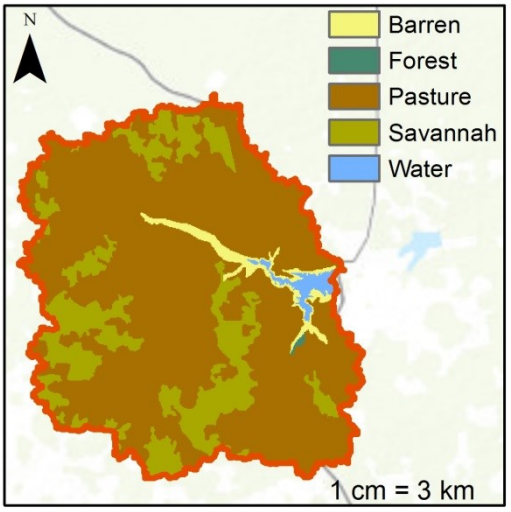

Figure 11: Land cover in the Tandjari watershed. AEG (2016)

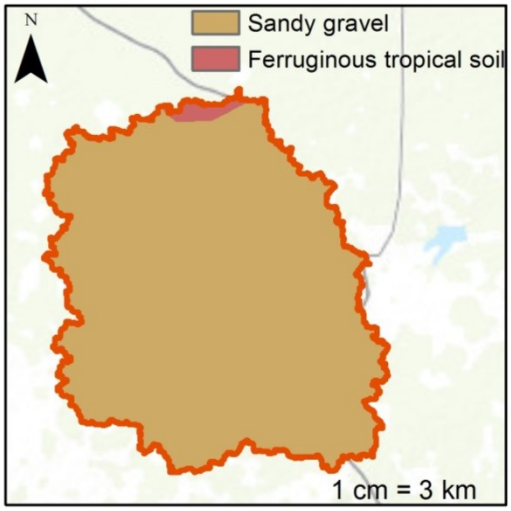

Figure 10: Major soils in the Tandjari watershed AEG (2016) (ESRI et al., 2016-2)

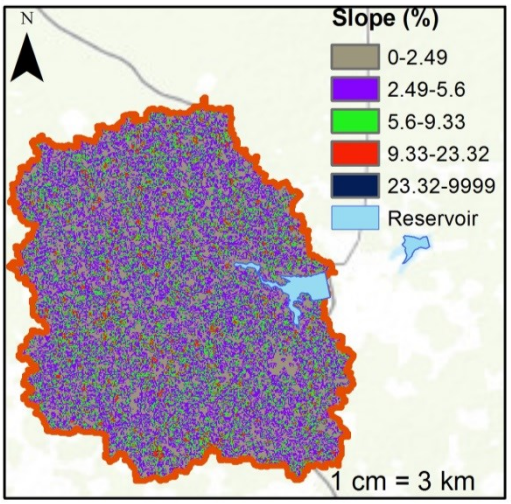

Figure 12: Slope map based on DEM (NASA et al., 2015) (ESRI et al., 2016-2)

Table 3: Soil parameters. Made available by Wellens (2016).

Parameters						
SNAM	FLTC				PEEL	
NLAYERS	4				2	
Data soil profile						
Layer thickness (cm)	0-22	22-48	48-71	71-110	0-6	6-11
Clay (%)	9.8	35.29	37.25	37.25	5.88	7.84
Silt (%)	52.95	41.18	39.22	43.14	27.45	19.61
Sand (%)	37.25	23.53	23.53	19.61	66.67	72.55
Rock (%)	2.12	<0,01	<0,01	<0,01	0.37	9.57
Soil water (mm)	49.52	13.79	12.32	23.07	6.54	6.39
MO totale (%)	0.78	1.66	0.4	0.48	0.97	0.79
C org. Total (%)	0.45	0.96	0.23	0.28	0.56	0.46
Total thickness (mm)	220	480	710	1100	60	110
Thickness layer (mm)	220	260	230	390	60	50
GLOBAL						
TEXT. Layer	Silt Loam	Clay Loam	Clay Loam	Silty Clay Loam	Sandy Loam	Sandy Loam
HYDRO. Layer	B	D	D	D	A	A
TEXTURE						
HYDGRP	D				A	
SOL_ZMX	1100	-	-	-	110	-
ANION_EXCL	0.5	-	-	-	0.5	-
SOL_CRK	0.5	-	-	-	0.5	-
LAYER						
SOL_Z	220	480	710	1100	60	110
SOL_BD	1.35	1.28	1.27	1.26	1.42	1.43
SOL_AWC	0.23	0.05	0.05	0.06	0.11	0.13
Ksat (cm/h)	2.8	0.32	0.28	0.31	4.8	3.83
SOL_K	28	3.2	2.8	3.1	48	38.3
SOL_CBN	0.45	0.96	0.23	0.28	0.56	0.46
CLAY	9.8	35.29	37.25	37.25	5.88	7.84
SILT	52.95	41.18	39.22	43.14	27.45	19.61
SAND	37.25	23.53	23.53	19.61	66.67	72.55
ROCK	0.0212	0	0	0	0.0037	0.0957
SOL_ALB	0.1	0.1	0.1	0.1	0.1	0.1
f_csand	0.2034				0.2000	
f_cl-si	0.9503				0.9434	
f_org	0.9990				0.9983	
f_hisand	0.9999				0.9731	
USLE_K	0.1931				0.1833	
SOL_EC	0	0	0	0	0	0
SOL_CAL	0	0	0	0	0	0
SOL_PH	7	7	7	7	7	7

Table 4: HRU distribution in the Tandjari watershed

		%age of catchment area (%)
Soils		
	Sandy gravel (PEEL)	99.3
	Ferruginous tropical soil (FLTC)	0.7
Land cover		
	Pasture, dryland, and cropland	83.2
	Savannah	15.9
	Barren	0.8
	Water	0.1
Slope		
	2.49 – 5.6	43.1
	5.6 - 9.33	22.8
	0 - 2.49	34.1

4.1.2 Weather data analysis

The graphs below show daily weather statistics of rainfall, maximum and minimum temperatures, average daily wind speed, relative humidity and solar radiation that were used as input data for the model. From January 2016 to April 2016 the DGM could not deliver weather data. These data gaps were covered, in the SWAT model, by generated weather data for which the program WXGEN was used (Sharpley and Williams, 1990).

The rainfall statistics show that 2012 and 2014 were average years with an annual rainfall of respectively 824 and 827 mm. In 2012 the total rainfall, of 797 mm, was 3.75 % below the average annual rainfall (828mm) and in 2015 the total rainfall was, with 844 mm, 2% above the average. A total number of 68, 67, 76, and 75 rainy days with maximum daily rainfalls of respectively 91 (August), 67 (April), 60 (September), 76 (August), and 44 (June) were observed in respectively 2012, 2013, 2014, 2015 and 2016. The highest monthly rainfall amount occurred in August in 2012 and 2015, in July in 2013 and 2016, and in September in 2014. The statistics of 2016 represent the consensus among farmers, who noticed that the rainy season arrived late in 2016.

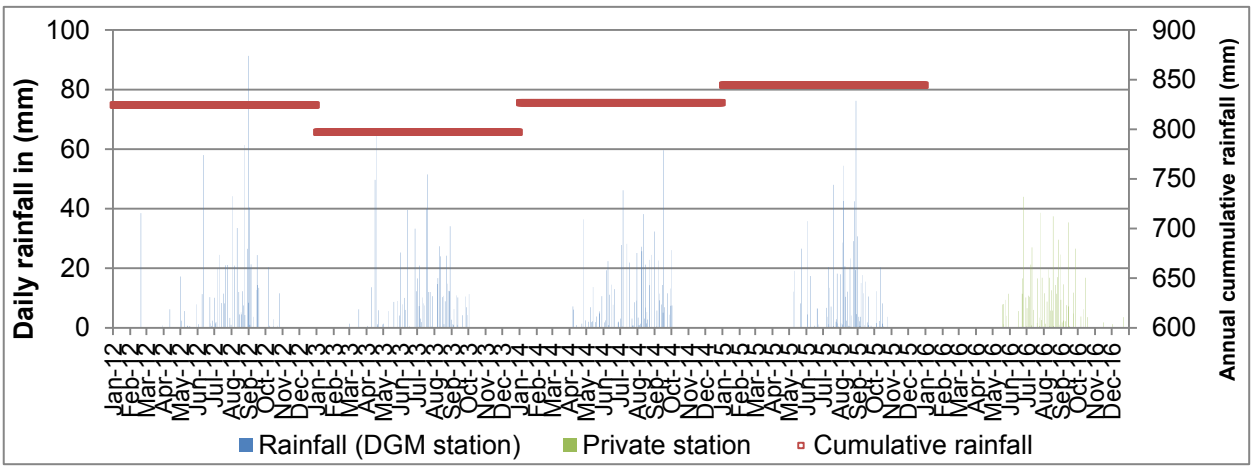

Figure 13: Rainfall measurements

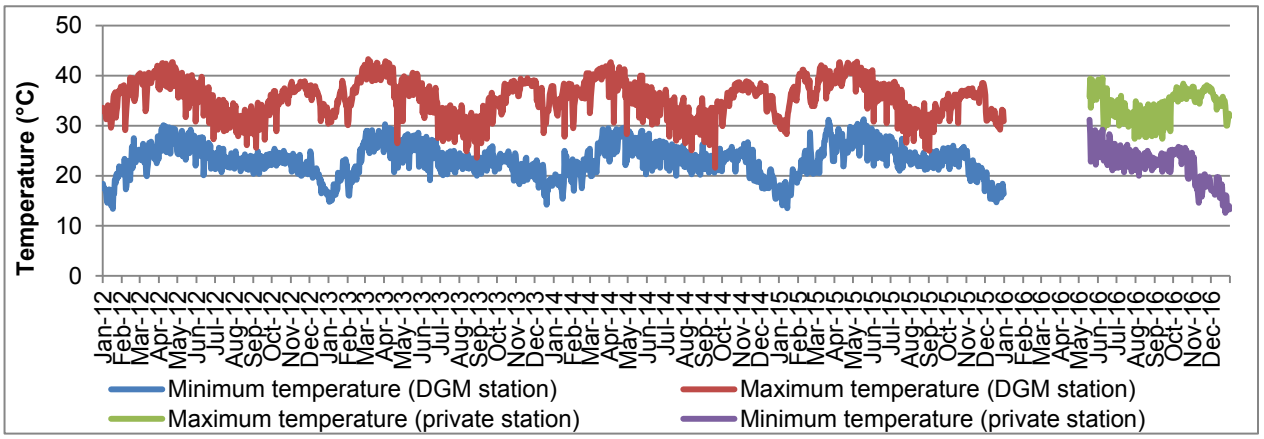

Figure 14: Temperature measurements

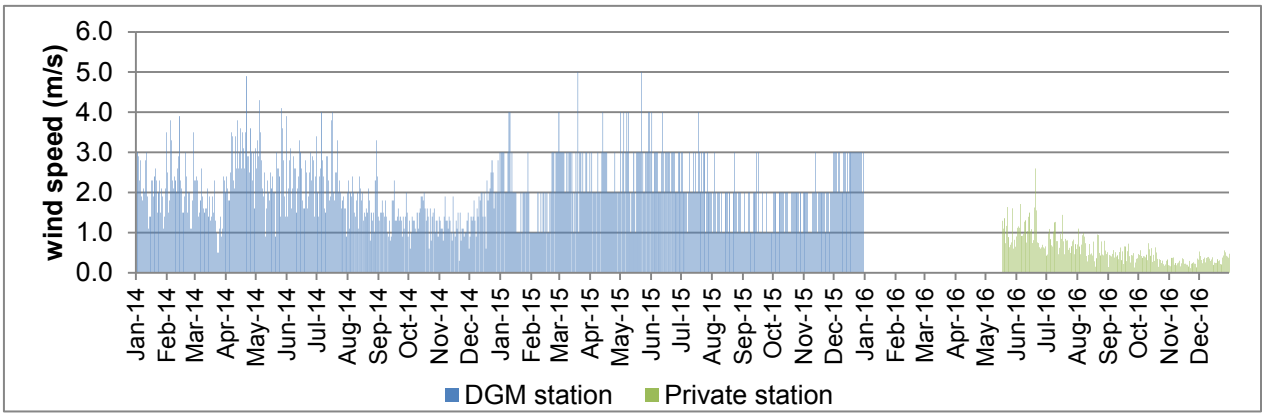

Figure 15: Wind speed measurements

Wind speed measurements up to 2014 were absent and were generated with the weather generator program WXGEN (Sharpley and Williams, 1990). From the wind observations it should be noticed that wind speed was structurally lower from the private weather station observations. This can be explained by the different setup of the anemometers. Due to safety reasons the private weather station, including the anemometer, had to be placed at the pump house of the ONEA, which was just after the dam, hence in the lee. Moreover the private station was located at 2 meters above the surface while the anemometer of the DGM was located 10 meters above surface.

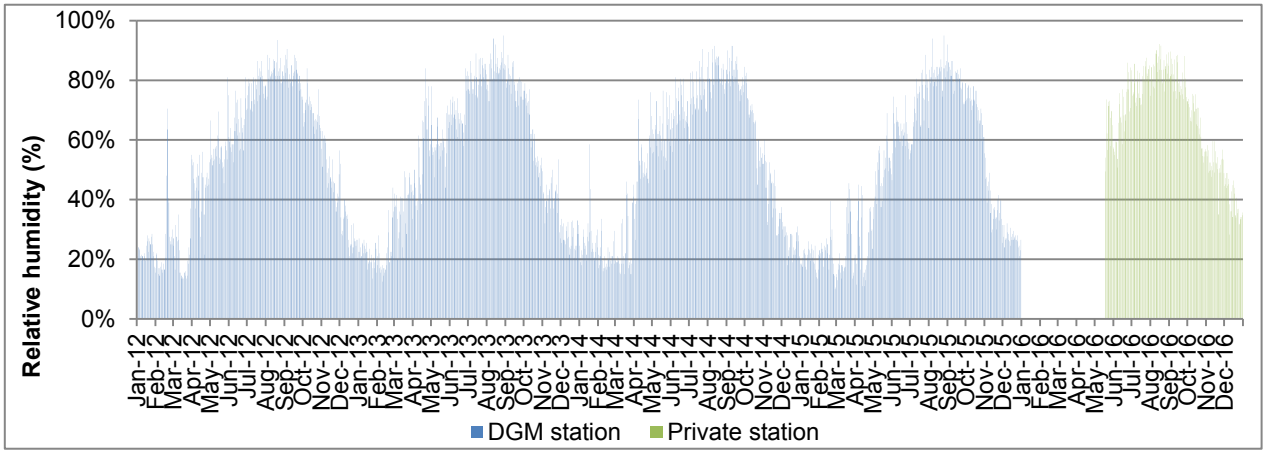

Figure 16 Temperature measurements

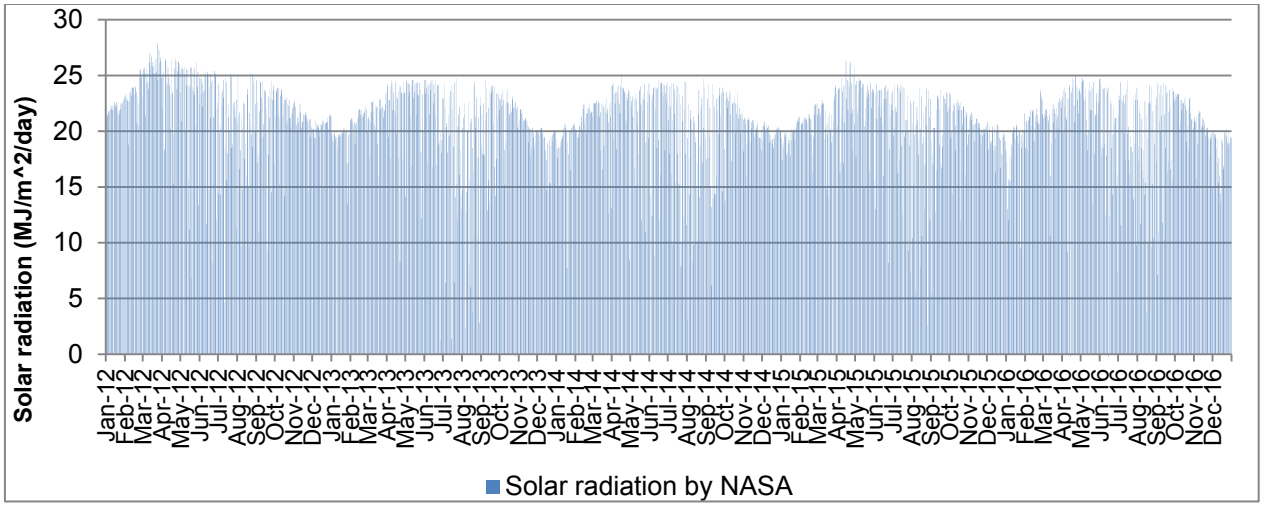

Figure 17: Daily averaged solar radiation based on data by NASA (Stackhouse, 2017)

4.1.3 Hydraulic conductivity of the reservoir bottom

In total five infiltration experiments were conducted at different locations on the land near the shore of the reservoir. In figure 18 the locations are projected on a satellite image taken in July 2012. Because water levels of the reservoir were low during the field work period it was possible to enter parts of the reservoir's bottom that would otherwise be under water, like on the satellite picture from 2012.

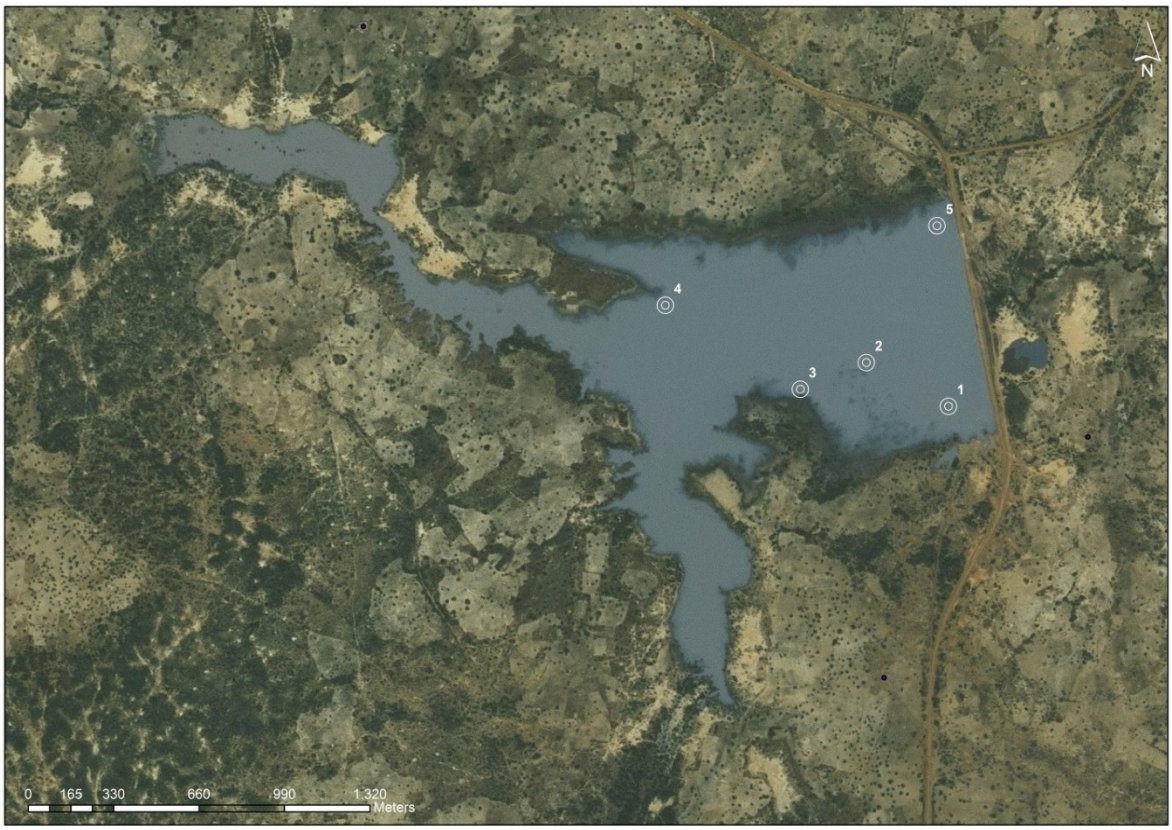

Figure 18: Locations of infiltration measurements carried out in May and June 2016 projected on Bing imagery taken from July 2012.

By sensory perception of the top soil, i.e. seeing (using a sand ruler), feeling and tasting, it was determined that the topsoil at all five locations consisted of sandy clay. As measurements took place close to the waterline the subsurface was already in near-saturated state. This is reflected by the results since a steady infiltration rate was rather quickly reached. Nevertheless, a long time span was chosen for each measurement since infiltration rates were in the order of millimeters per hour, which made readings from the Mariotte bottle for small amounts of infiltration difficult, and hence a longer time allowed the readings to be more accurate. Figure 19 to 23 show the cumulative infiltration and the infiltration rates for the experiment on the different locations. From location 1, 2 and 5 can be noticed that the water infiltrated somewhat faster in the beginning after which the infiltration rate decreased to a rather constant value. This constant value is called the basic infiltration rate and is approximately equal to the near-saturated permeability. The fully saturated hydraulic conductivity K_{sat} has a slightly lower value and is obtained by using a constant equal to (2/3). These calculated K_{sat} values are presented in table 5. At location 1 and 2 the saturated hydraulic conductivity (K_{sat}) was in the order of millimeters per hour while at the locations 3 and 5 the K_{sat} was in the order of a tenth millimeter per hour. The measured K_{sat} at location 4 shows, with a of 24,1 mm/h (equal to 0.58m/day), a large deviation from the other results. The boxplot in figure 24 makes the degree of spreading of the five data points more clear. 50% of the data fall within the box and the whiskers show the most extreme data points which are respectively 24,1 mm/h and 0,2 mm/h. Value 24,1 is considered as an outlier and was therefore not taken into account for the determined average K_{sat} value.

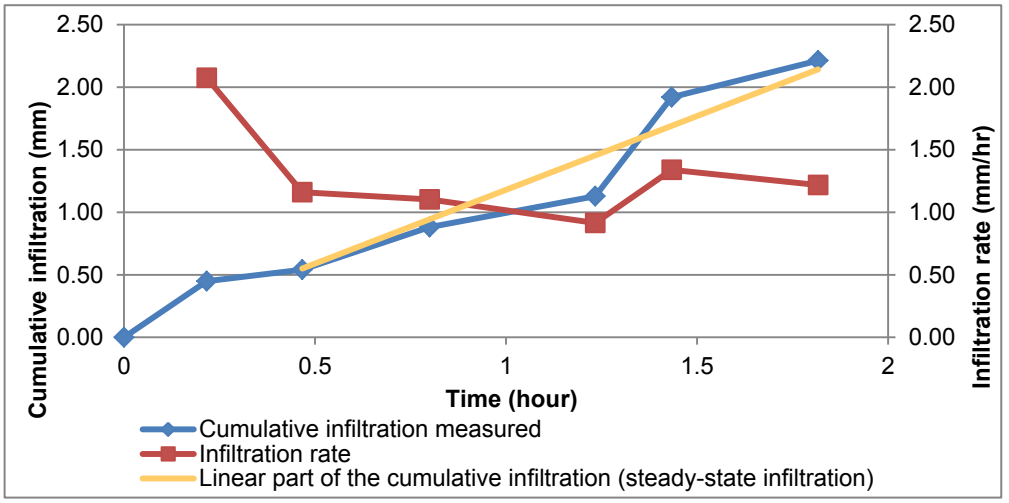

Figure 19: Cumulative infiltration and infiltration rate at location 1

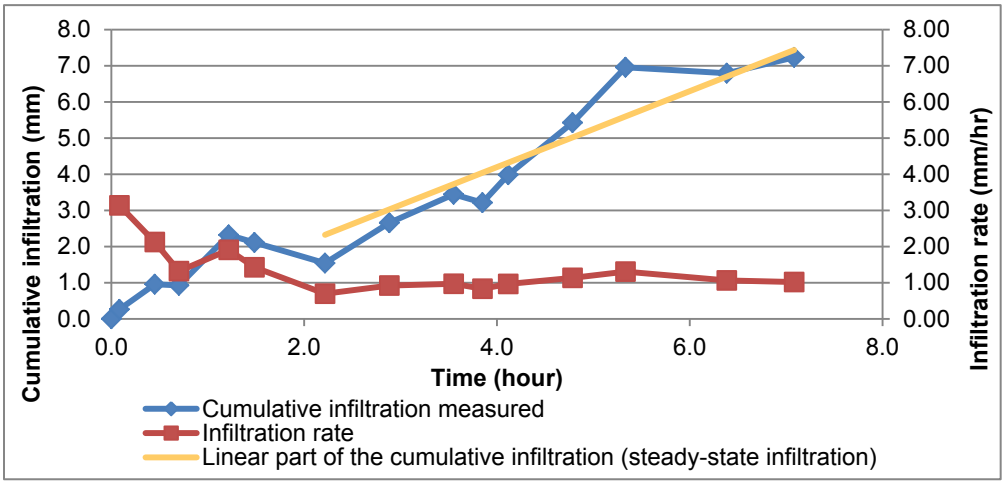

Figure 20: Cumulative infiltration and infiltration rate at location 2

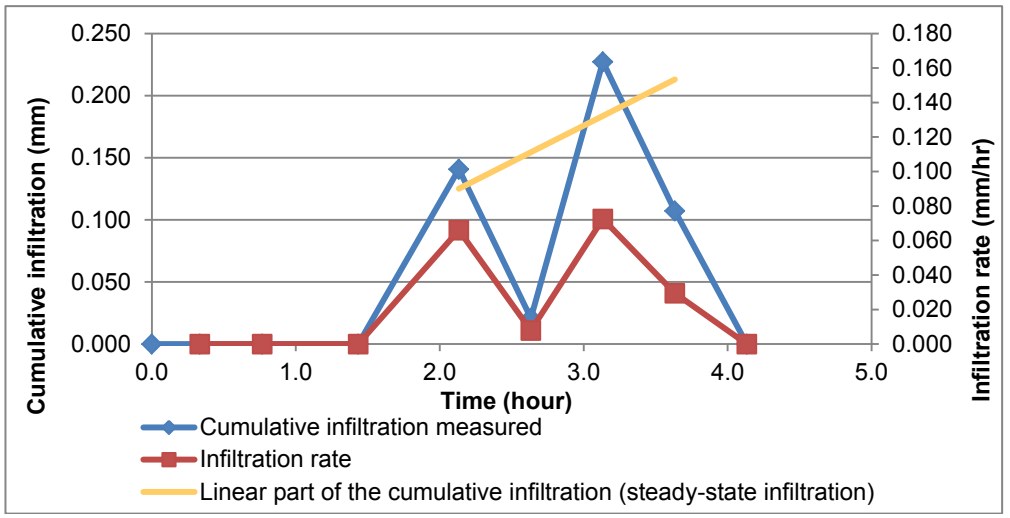

Figure 21: Cumulative infiltration and infiltration rate at location 3

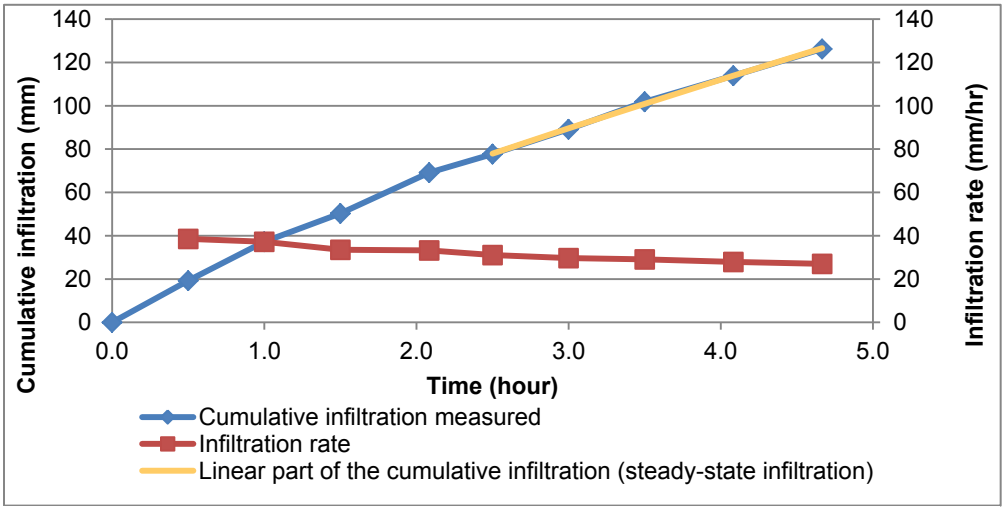

Figure 22: Cumulative infiltration and infiltration rate at location 4

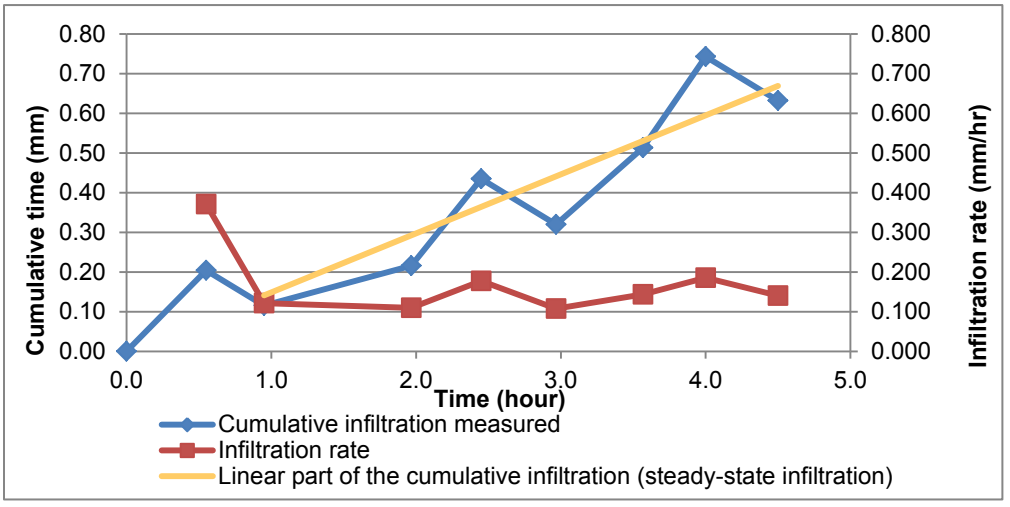

Figure 23: Cumulative infiltration and infiltration rate at location 5

Table 5: Values for nearly saturated hydraulic conductivity (K_{sat}) of the infiltrometer experiment at five different locations near the Tandjari reservoir's shoreline

Locations	Saturated hydraulic conductivity (mm/h)
1	1.8
2	1.6
3	0.1
4	24.1
5	0.2

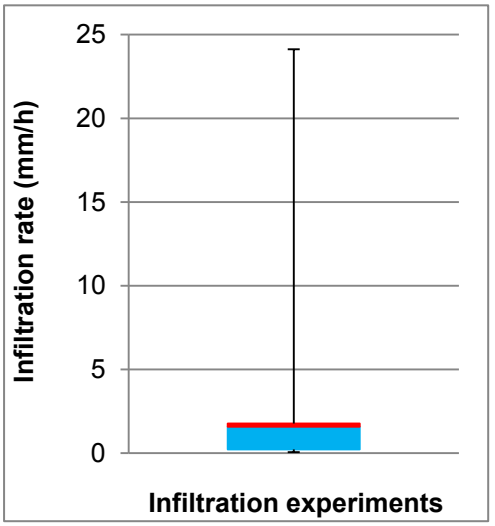

Figure 24 Boxplot of the infiltration data series

The average saturated hydraulic conductivity (K_{sat}) of the reservoir bottom, taken into account locations 1,2,3 and 5 is ***0.9 mm/h.*** This value was used in the initial simulation by the model to calculate the volume that infiltrated in the reservoir bottom.

4.1.4 Water consumption

In this section, the collected data with regard to monthly water consumption from the reservoir are presented. Section 4.1.2.1 describes the data of water withdrawals from the reservoir by drinking water company ONEA. Section 4.1.2.2 describes the estimated water use by livestock. Section 4.1.2.3 discusses the results of the data collection on domestic water use. In section 4.1.3.4 irrigation data is presented. The last section 4.1.3.5 gives an overview of the total monthly water consumption from the Tandjari reservoir.

4.1.4.1 Water abstraction by the drinking water company ONEA

The drinking water company ONEA is using two pumps, with capacities of 90 $m^3\ hr^{-1}$ and 120 $m^3\ hr^{-1}$, for the intake of water from the Tandjari reservoir. The water is transported to a water treatment plant in Fada N'Gourma after which it is distributed to the consumers in the city. ONEA is currently running their treatment plant at maximum capacity of 100 $m^3\ hr^{-1}$. The drinking water company wants to keep up with the growing water demand, due to population growth and rising living standards, and is therefore planning to scale up the treatment plant's capacity by installing an additional pump at the water intake with a capacity of 120 $m^3\ h^{-1}$ (Chanoine, 2016).

Figure 25 presents the monthly water abstraction from the Tandjari reservoir by the drinking water company. In 2012 and 2014 the average monthly abstraction was respectively 42 and 43 thousand cubic meters. From April 2015 it can be noticed that the water intake has increased, which resulted in an average monthly water intake of 53 thousand cubic meters in 2015 and for the first months in 2016 this was 63 thousand cubic meters. In total 640 thousand cubic meters of water was abstracted in 2015 (ONEA, 2016).

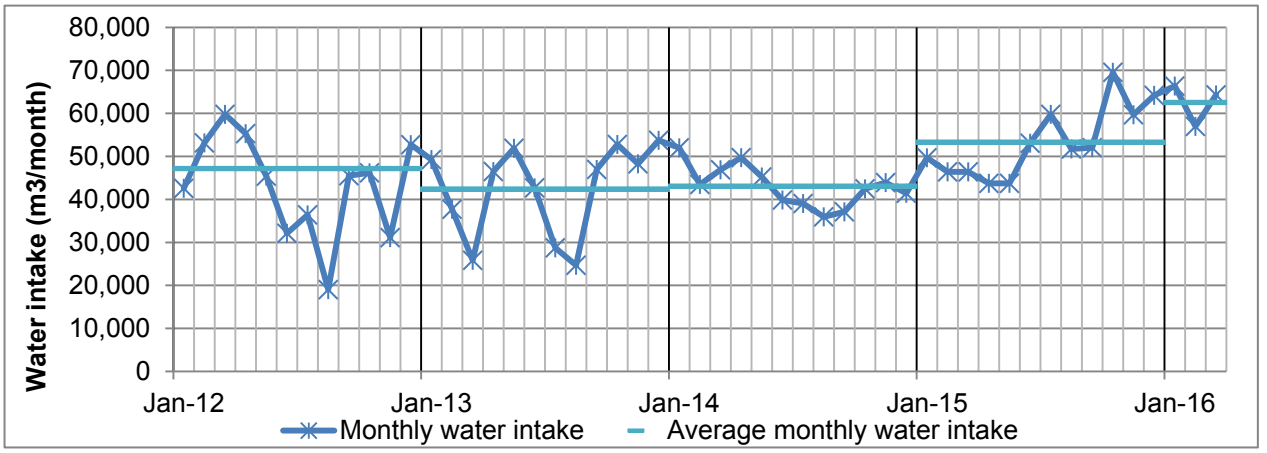

Figure 25: Monthly water intake from the Tandjari reservoir by the drinking water company (ONEA, 2016)

Since 2006 the population in Fada N'Gourma has grown steadily with an annual average growth rate of 3,4% (l'Institut National de la & Démographie, 2016). Based on this growth rate and the most recent population census (Central Office of the Census, 2006) the population is currently estimated at 60 thousand (O. Chanoine, personal communication, May 12, 2016). It is assumed that the annual growth of 3,4% will continue in the years to come. Based on this assumption the population in Fada N'Gourma is expected to approach 100 thousand people in 2030.

With the growing population the demand for water will increase significantly as well. This forecasted demand is calculated by using drinking water guidelines. The United Nations has set the guideline for the water demand to 20 liters per capita per day for basic needs (WHO & Unicef, 2000), although the ONEA strives to deliver 37 liters per capita per day. As can be seen from figure 26, the ONEA has met the guideline of United Nations, except from few drops below the line in 2012 and 2013. The water company did not succeed in meeting their own guideline (37 liters/capita/day) up to 2015. However, since October 2015 the water supply is in line with their guideline. When the water demand is extrapolated, using the ONEA guideline, it will be nearly doubled by 2030; approximately 110 thousand cubic meters per month.

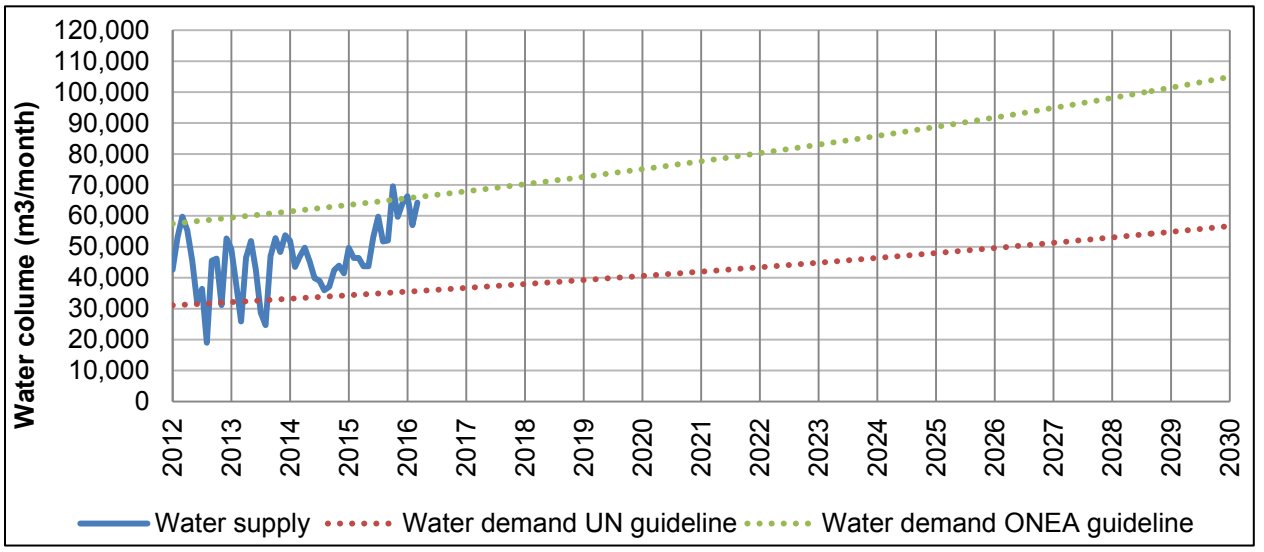

Figure 26: Prediction of water demand until 2030 for Fada N'Gourma

4.1.4.2 Water consumption by livestock

Based on the most recent livestock census, which was carried out in 2003 by the Ministry of Animal Resources in the districts of Yamba and Fada N'Gourma, the livestock population in subsequent years in the catchment area of the Tandjari reservoir is determined[1]. Based on the ratio catchment area/district area, the numbers of animals in the catchment area of the Tandjari reservoir were calculated. Annual livestock population growth numbers consisting of two % for bovine, asinus and procine, three % for ovine and caprine, and one % for equine, were used to estimate the current (2016) and the prospected livestock population in 2030 (Ministere des Ressources Animales, 2003) (table 6). Furthermore it is assumed that the livestock in the Tandjari catchment is using the reservoir for their drinking water needs year-round. In table 6, the statistics of the livestock census in 2003 are presented. In table 7, the livestock population in the Tandari catchment and its associated water consumption in 2016 and the prospected water consumption in 2030 are presented.

Table 6: Situation of livestock in 2003 in Yamba, Fada N'Gourma and the Tandjari reservoir's watershed
After: (Ministere des Ressources Animales, 2003)

Situation of livestock in 2003, province gourma								
Region	Bovine	Ovine	Caprine	Porcine	Asinus	Equine	area district (km2)	percentage of area in watershed (%)
Fada N'Gourma	24014	21901	28641	5703	3418	66	3439	1.08
Yamba district	8875	8094	10585	2108	1263	24	1407	4.83
Fada N'Gourma	258	236	308	61	37	1	37	
Yamba part of the	429	391	512	102	61	1	68	
Watershed total	687	627	820	163	98	2	105	

Table 7: Water consumption by livestock
* (Ministere des Ressources Animales, 2003) ** (Lhoste, Dollé, Rousseau, & Soltner, 1993)

Water consumption by livestock anno 2016					**Water consumption by livestock prospection 2030**			
Animal group	**Percentage**	**Total number of animals ***	**Consumption by animal group (L/day) ****	**Total consumption (m3/month)**	**Percentage**	**Total number of animals ***	**Consumption by animal group (L/day) ****	**Total consumption (m3/month)**
Bovine	27%	890	40	1,080	20%	900	40	1090
Caprine	36%	1200	4	150	40%	1820	4	220
Ovine	27%	920	4	110	31%	1390	4	170
Asinus	4%	130	13	50	4%	170	13	70
Porcine	6%	210	5	30	6%	280	5	40
Equine	0%	0	30	-	0%	0	30	0
Total	100%	3350	66	1420	100%	4560	66	1593

4.1.4.3 Domestic water use

The domestic water use estimation is based on field observations and the latest population census that was carried out in 2006 including the villages that are situated in the catchment area of the Tandjari reservoir. In order to determine the current population a yearly rural population growth of 3.1% was assumed (l'Institut National de la & Démographie, 2006). Based on field observations it was estimated that on average 100 lorries with jerrycans were daily filled with water and that an average lorry transports 250 liters of water. From interviews it became clear

[1] A new animal census is scheduled for 2017.

that several wells were out of use so it was assumed that the villages Komandougou and Tandjari are fully dependent on the reservoir's water for their water needs where the villages Tankilounga and Komangou use wells for their water needs (refer to annex 6 for the complete results of the interviews). Based on these statistics the average water consumption from the reservoir per person per day in 2016, for the villages Komandougou and Tandjari with a total of 4624 inhabitants, is equivalent to approximately 5 liter per day per person. This 5 liter estimate is used to calculate the total water usage in cubic meters per month as presented in table 8.

Table 8: Water consumption from the Tandjari reservoir for domestic usage.
** (l'Institut National de la & Démographie, 2006) ** (Ministere de l'Eau des Amenagements Hydrauliques et de l'Assainissement, 2015). *** (Adjina, 2016), (Ladja, 2016), (Woba, 2016), (Sougoulingo, 2016).*

	Komandougou	**Tankilounga**	**Tandjari**	**Komangou**	**Total**
Population (2006) *	1456	900	1951	1577	5884
Population 2016 (estimation)	1976	1221	2648	2140	7985
Population 2030 (estimation)	3029	1873	4059	3281	12243
Number of wells official data **	7	1	7	5	
Number of wells from interviews ***	0	2	0	2	
Estimated water consumption (L/day/person)	5.4	0	5.4	0	
Domestic water consumation anno 2016 (m3/month)	320	0	440	0	**760**
Domestic water consumation anno 2030 (m3/month)	500	0	670	0	**1170**
Interviewee	Bongo Adjina	Lompo Ladja	Thomas Woba	Ouoba Sougoulingo	

4.1.4.4 Irrigation

Irrigation data was made available by the Department of Agriculture (Lompo, 2016). Ten % of total catchment area is used for cultivating crops including millet, sorghum, peanuts, cassava, tomatoes, zucchini and rice. At the north side of the reservoir there are five to six hectares of cultivated land that are operated by 50 farmers. On the south side of the reservoir, two hectares of land are cultivated with a total of 30 operators (figure 27). Irrigation of the land by in total 19 moto pumps, with a pump capacity of 60 cubic meters per hour, takes place from December to March up to 3 times a week for maximal 3 hours at a time (table 9). In addition a rice farmer, who is growing rice year-round, is irrigating once per day for a maximum of three hours.

Table 9: Water abstraction from the Tandjari reservoir by irrigation

Month	**Irrigated water (m3/month)**
January	46521
February	46521
March	46521
April	5481
May	5481
June	5481
July	5481
August	5481
September	5481
October	5481
November	5481
December	46521

legend	
	Irrigation various crops
	Only irrigation of rice fields

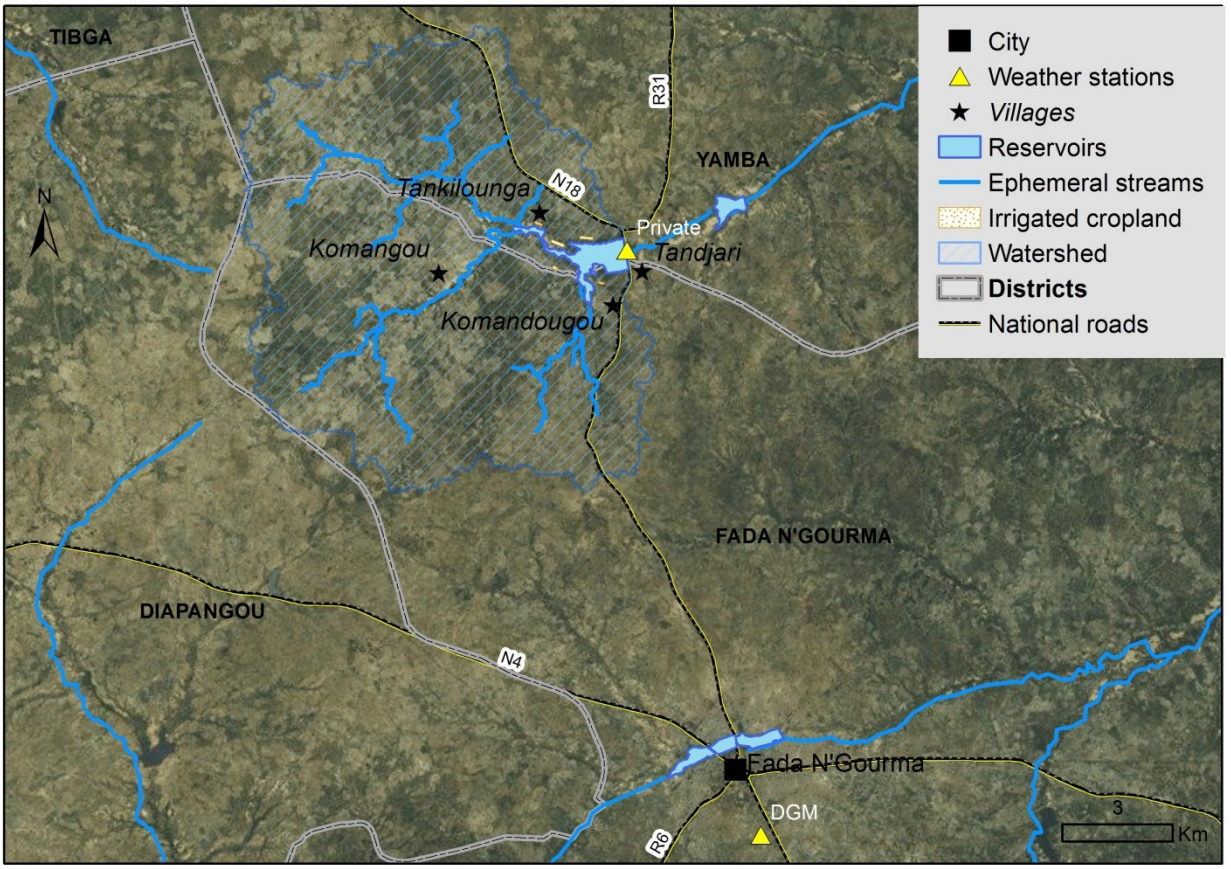

Figure 27: Irrigated cropland and villages in the Tandjari Watershed. (Esri et al., 2016-2)

4.1.4.5 Total water consumption

In table 10 the monthly water consumption from the Tandjari reservoir in 2016 and the forecasted water consumption in 2030 are presented. The values that are given in cubic meters are rounded to hundredths. The pie charts in figure 28 give an overview of the annual water consumption in 2016 by different water users. The drinking water company ONEA is with 69 % of the total water use, the largest consumer. Farmers represent the second largest user group by consuming 29% of the total water usage for irrigation and for drinking water for their livestock, which are separately accounting for respectively 27% and two%. The least water is used for domestic purposes by the inhabitants of the surrounding rural villages accounting for one% of the total water usage.

Table 10: Monthly water consumption from the Tandjari reservoir for 2016 (left) and 2030 (right). Nota bene values are rounded to the nearest hundred.

Water consumption in cubicmeters anno 2016					
	Water supply	**Livestock**	**Domestic**	**Irrigation**	**Total**
January	65,000	1,400	800	46,500	113,700
February	47,600	1,400	800	46,500	96,300
March	60,800	1,400	800	46,500	109,500
April	48,800	1,400	800	5,500	56,500
May	46,600	1,400	800	5,500	54,300
June	41,900	1,400	800	5,500	49,600
July	41,000	1,400	800	5,500	48,700
August	32,800	1,400	800	5,500	40,500
September	45,400	1,400	800	5,500	53,100
October	52,700	1,400	800	5,500	60,400
November	45,800	1,400	800	5,500	53,500
December	53,000	1,400	800	46,500	101,700
Total	581,400	16,800	9,600	230,000	837,800
Precentage	69.4%	2.0%	1.1%	27.5%	100.00%

Water consumptionin cubicmeters anno 2030					
Water supply	**Livestock**	**Domestic**	**Irrigation**	**Total**	
104,900	1,600	1,200	46,500	154,200	
105,200	1,600	1,200	46,500	154,500	
105,500	1,600	1,200	46,500	154,800	
105,800	1,600	1,200	5,500	114,100	
106,100	1,600	1,200	5,500	114,400	
106,400	1,600	1,200	5,500	114,700	
106,700	1,600	1,200	5,500	115,000	
107,000	1,600	1,200	5,500	115,300	
107,300	1,600	1,200	5,500	115,600	
107,600	1,600	1,200	5,500	115,900	
107,900	1,600	1,200	5,500	116,200	
108,200	1,600	1,200	46,500	157,500	
1,278,400	19,100	14,000	229,900	1,541,400	
82.9%	1.2%	0.9%	14.9%	100%	

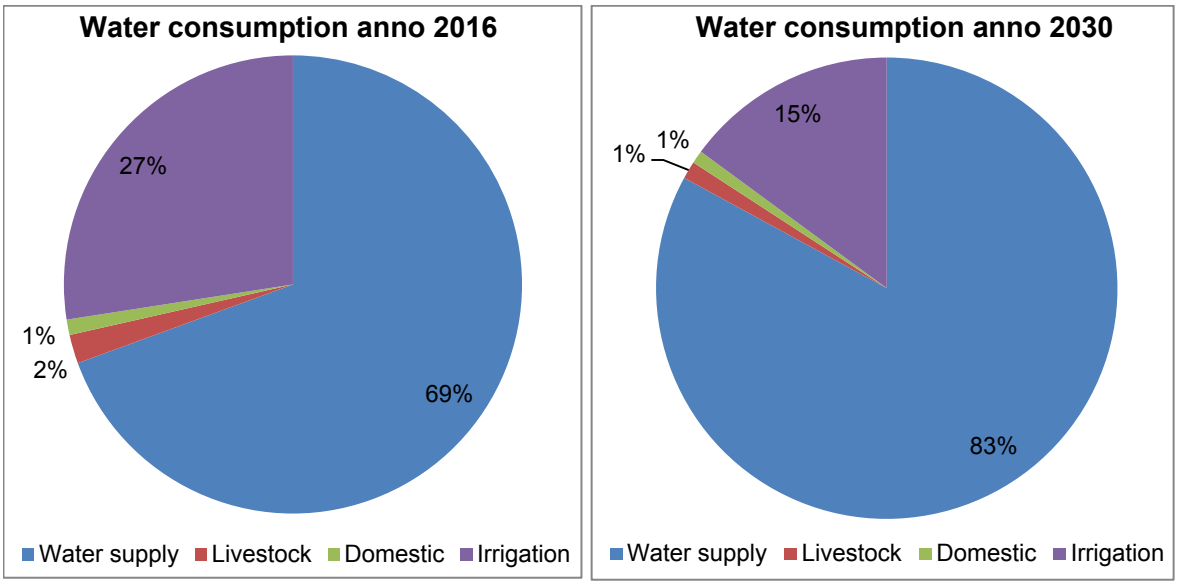

Figure 28: Water consumption distribution for the Tandjari reservoir

4.2 Observed reservoir storage

From February 2012 to April 2015 the ONEA has taken monthly records of the reservoir water levels, as shown in table 11. In May 2016 the readings resumed with a data logger that registered water levels with a sub-daily time interval. Given the water levels, the reservoir volume and surface area were derived by using the water level-volume and area-volume relations, which were obtained from the bathymetry data (SEREIN-GE SARL, 2014). Reservoir volumes from February 2012 to April 2015 and June 2016 to December 2016 as well as monthly rainfall values for the four years are shown in figure 29. Also the critical reservoir volume at the lowest point of the water intake and the maximum reservoir volume at spillway level are indicated. 38 months of observed data, from 2012 to February 2015, were used for calibration and the remaining 8 months of data, from May 2016 to December 2016, were used for validation.

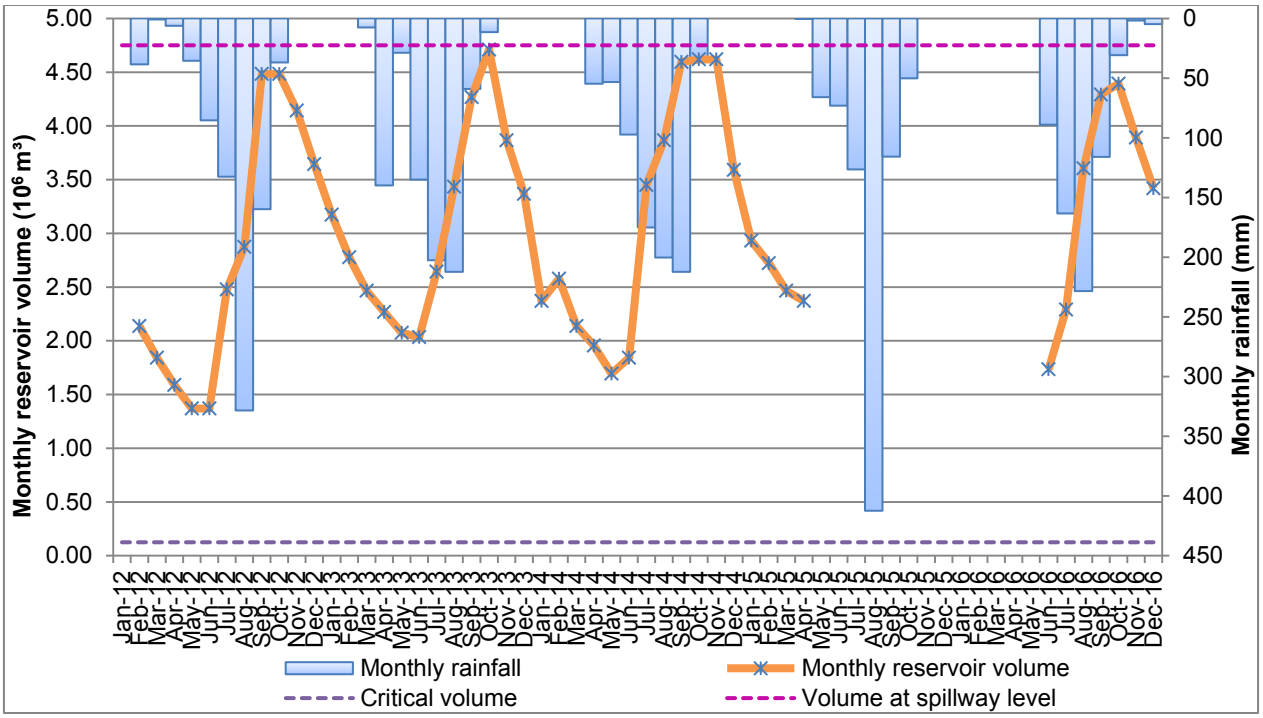

Figure 29: Monthly reservoir volumes and rainfall from January 2016 to December 2016. Note: Reservoir volumes from May 2015 to March 2015 are missing.

Minimum reservoir volumes were observed at the end of the dry season in May. From the start of the rainy season in June the reservoir fills up and reaches maximum storage volumes in August and September. In 2013 the maximum reservoir storage of 4.7 million cubic meters (at 6.47m) was recorded. It should be noted that despite that measurements did not recorded maximum water levels (6.47 m) in the other years, it does not necessarily imply the maximum level was not reached, because a monthly interval of water level readings is insufficient to determine this with certainty.

Table 11: Reservoir water levels and associating reservoir volume and surface area (ONEA, 2016)

Measured water levels by ONEA (m) (reconstructed)					
month/year	Start month (m)	End month (m)	Difference (m)	Volume (m3)	Surface (ha)
Jan-12	-	-	-	-	-
Feb-12	4.9	4.6	-0.3	2,136,700	110
Mar-12	4.6	4.3	-0.3	1,842,400	90
Apr-12	4.3	4	-0.3	1,588,600	90
May-12	4	4	0	1,369,700	80
Jun-12	4	5.2	1.2	1,369,700	80
Jul-12	5.2	5.5	0.3	2,478,200	120
Aug-12	5.5	6.4	0.9	2,874,100	140
Sep-12	6.4	6.4	0	4,483,600	220
Oct-12	6.4	6.24	-0.16	4,483,600	220
Nov-12	6.24	5.98	-0.26	4,142,800	200
Dec-12	5.98	5.7	-0.28	3,643,400	170
Jan-13	5.7	5.43	-0.27	3,172,600	150
Feb-13	5.43	5.19	-0.24	2,776,400	130
Mar-13	5.19	5.02	-0.17	2,465,900	120
Apr-13	5.02	4.84	-0.18	2,267,300	110
May-13	4.84	4.8	-0.04	2,074,300	100
Jun-13	4.8	5.33	0.53	2,033,700	100
Jul-13	5.33	5.86	0.53	2,642,600	130
Aug-13	5.86	6.3	0.44	3,433,600	160
Sep-13	6.3	6.5	0.2	4,267,500	210
Oct-13	6.5	6.1	-0.4	4,710,700	230
Nov-13	6.1	5.82	-0.28	3,865,900	190
Dec-13	5.82	5.1	-0.72	3,366,400	160
Jan-14	5.11	5.28	0.17	2,370,400	110
Feb-14	5.28	4.9	-0.38	2,578,100	120
Mar-14	4.9	4.72	-0.18	2,136,700	110
Apr-14	4.72	4.43	-0.29	1,954,900	100
May-14	4.43	4.6	0.17	1,693,900	90
Jun-14	4.6	5.87	1.27	1,842,400	90
Jul-14	5.87	6.1	0.23	3,450,600	160
Aug-14	6.1	6.45	0.35	3,865,900	190
Sep-14	6.45	6.46	0.01	4,595,800	230
Oct-14	6.46	6.45	-0.01	4,618,500	230
Nov-14	6.46	5.95	-0.51	4,618,500	230
Dec-14	5.95	5.54	-0.41	3,589,800	170
Jan-15	5.54	5.39	-0.15	2,931,500	140
Feb-15	5.39	5.19	-0.2	2,722,100	130
Mar-15	5.19	5.11	-0.08	2,465,900	120
Apr-15	5.11	5.2	0.09	2,370,400	110
May-15	no data				
Jun-15	no data				
Jul-15	no data				
Aug-15	no data				
Sep-15	no data				
Oct-15	no data				
Nov-15	no data				
Dec-15	no data				
Jan-16	no data				
Feb-16	no data				
Mar-16	no data				
Apr-16	no data				
May-16	no data				
Jun-16	4.48	5.04	0.56292	1,734,596	87
Jul-16	5.04	5.96	0.91758	2,290,827	108
Aug-16	5.96	6.31	0.35292	3,604,883	177
Sep-16	6.31	6.36	0.04725	4,291,632	209
Oct-16	6.36	6.11	-0.24559	4,393,004	213
Nov-16	6.11	5.85	-0.26191	3,891,005	191
Dec-16	5.85	5.61	-0.24267	3,418,691	167

Figure 30 shows the water levels recordings from the diver and the daily rainfall recordings from the private weather station (figure 27), from May 25, 2016 to December 16, 2016. The maximum water level was reached on the 26th of September, when it was at spillway level. The minimum level of 304.2 meters was observed on June 21, 2016. This level was well above the critical level of 301.4 meters, which is equal to a reservoir storage of 125 000 cubic meters (SARL, 2014). When the critical level is exceeded, the water intake pipe is not submerged anymore which would interrupt the water supply to the water treatment plant in Fada N'Gourma.

The response of the filling curve to rainfall shows that low rains (5-10mm/day) were not likely to generate runoff in the upstream catchment area, according to the rainfall classification developed by Ibrahim et al. (2012). The moderate rains (10-20 mm/day) and strong rains (20-50 mm/day) on the other hand are followed by a significant increase in reservoir level, mainly due to the major contribution of the catchment by runoff generation. The observed pattern corresponds to the findings of Liebe *et al*. (2009) who determined that the contributing area increases with the size of the storm, hence, the more catchment area is contributing, the more runoff flows to the reservoir.

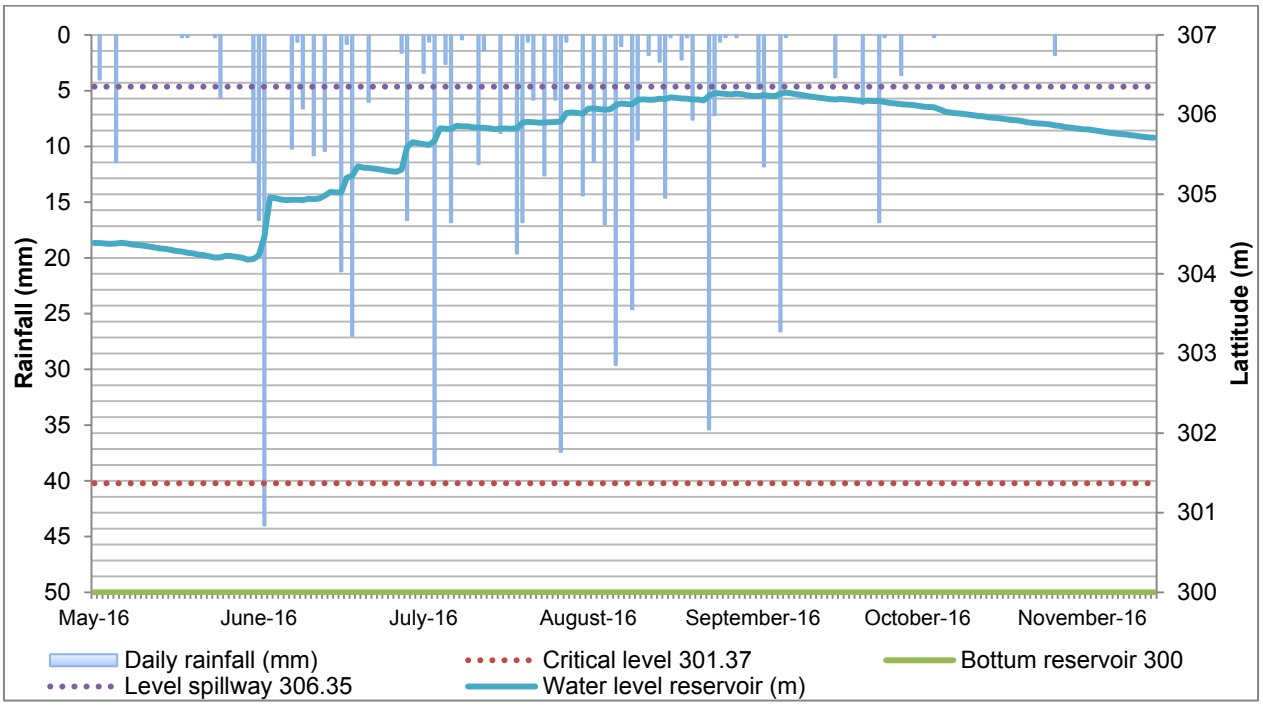

Figure 30: Water level measurements and the recorded rainfall may 2016 – October 2016

4.3 Sensitivity analysis

The results of the global sensitivity analysis are given in table 12. The table shows the sensitivities of the model parameters in descending order from most sensitive to least sensitive parameter, hence, the larger the absolute value of t-stat, and the smaller the p-value, the more sensitive the parameter. The model was most sensitive to the hydraulic conductivity of the reservoir (RES_K) bottom, followed by the reservoir evaporation coefficient (RES_EVRSV) and the runoff curve number (CN2). RES_K and RES_EVRS are directly related to the reservoir outflow by respectively infiltration and evaporation. The CN2 determines the first step in the water routing cycle by the subdivision of rainfall into runoff and infiltration. Hence, it has a significant impact on the reservoir water inflow from the catchment.

Table 12: Model parameters in descending order from most sensitive to least sensitive

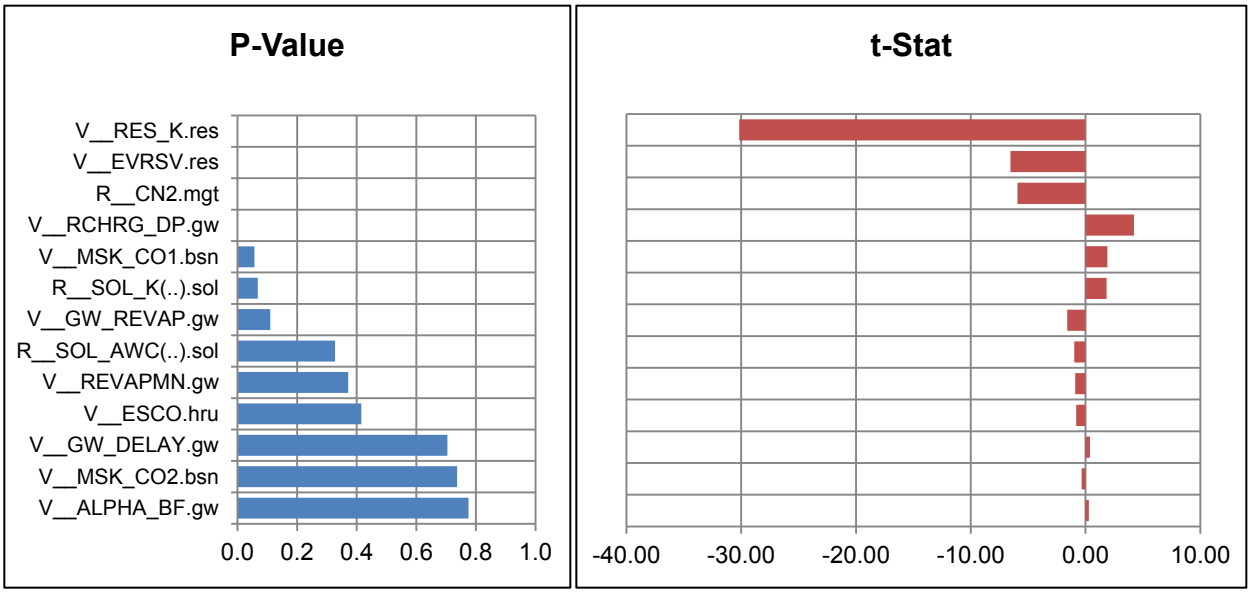

4.4 Calibration and validation

Calibration and validation were based on a comparison of observed reservoir storage (based on reservoir level measurements) against model simulations. For the calibration procedure weather data from the DGM weather station (see chapter 3.2.3) and observed data obtained from water level records of ONEA were used covering the period from February 2012 to March 2015. Validation was done with weather data obtained from the private weather station (see chapter 3.2.3) and observed data obtained from the private data logger records. Data from the latter, covered the period of May 2016 to December 2016.

The calibrated model showed that 62% of the simulated reservoir storage was within the 95PPU band, hence accounting for all the correct processes. The quality of the model, indicated by the thickness of the 95PPU band, referred to as the R-factor, was 0.49 (out of a perfect 0, but quite reasonable around 1). The performance of the calibrated model in terms of the Kling-Gupta

efficiency (KGE) and the coefficient of determination (R^2) of the best simulation, i.e. the simulation with the best parameter set, were respectively 0.83 and 0.70, which can be regarded as satisfactory. The PBIAS value of -0.0 % indicated that the model did not over- or underestimate the observed reservoir storage. A graphical representation of the observed versus simulated reservoir storage is presented in figure 31. As can be seen, the best simulation fitted the observed reservoir storage reasonably well, except from a mismatch in March 2013 when the model simulated an increase of reservoir storage while the observations showed a decline in reservoir storage. The system showed a response to a localized rain event in Fada N'Gourma (DGM station), which did not occur in the Tandjari catchment. This highlights the importance of gauged upstream catchments of reservoirs.

The validated model showed that the 95PPU band bracketed 75% of simulated data and the thickness of the band, indicated by the R-factor, was 0.44. The KGE and R^2 of the validated model were respectively 0.78 and 0.93. The improved behavioral parameters for the validated model indicate that the model reliability improved compared to the calibrated model. The improved model performance with the data set from the private weather station can be attributed to the better location of the private station with respect to the catchment. The private weather station is situated adjacent to the catchment, while the DGM is 15 km away from the catchment. Moreover, the observed reservoir data used in the validation procedure were obtained by automated water level recordings, which minimized errors due to human intervention.

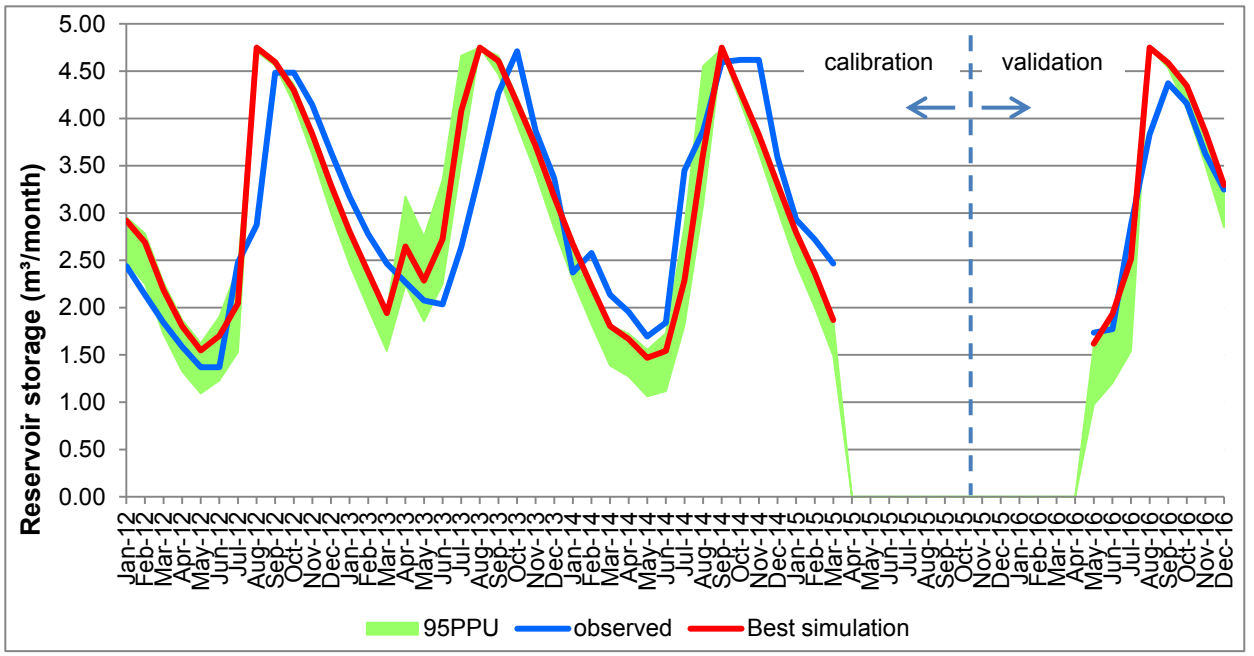

Figure 31: Best simulated (out of 500 simulations) (red line) and observed (blue line) monthly reservoir storage and the 95PPU band thickness of all variables. On the y-axis the reservoir storage in cubic meters per month and on the x-axis the consecutive months, starting from the first (1) month January 2012 and ending at the last simulated month (36) December 2014, are set out.

4.5 Water balance results

In this section the results of the various water balance components are explained in detail.

4.5.1 Reservoir inflow: runoff, groundwater inflow and direct rainfall

The unevenly distributed rainfall and large rainfall events resulted in high streamflow in the rainy season whereas streamflow was zero during most of the dry season. Both runoff and groundwater, upstream are feeding the ephemeral streams (fig. 26), which lead to the reservoir. The reservoir is also fed directly by runoff from the reservoir banks. The total average annual reservoir inflow by both runoff and groundwater inflow was 5.0 MCM accounting for 80 % of the total inflow, where the average rainfall on the reservoir surface amounted 1.3 MCM, covering the other 20% of the total inflow.

4.5.2 Evaporation losses

Annual evaporation losses ranged from 1.8 MCM in 2012 to 1.4 MCM in 2016. The average amount of water loss by evaporation was 1.6 MCM per year accounting for 43% the total water outflow. This is similar to the findings of Fowe et al. (2015) who estimated 40% average evaporation loss relative to the total outflow (water consumption volumes were similar as well) of the Boura reservoir in southern Burkina Faso.

4.5.3 Infiltration losses

The average amount of water loss by infiltration was 1.4 MCM per year accounting for 22% of the total water outflow. The average infiltration is about half the average reservoir evaporation. This means that on average 4.3 thousand cubic meters of water is leaving the reservoir each day.

The reservoir has thus an important secondary advantage of recharging regional aquifer(s). For the surrounding villages (8000 people live in the surroundings of the dam) the amount of annual average aquifer recharge by the reservoir is equal to 480 L per person per day. A part from the groundwater recharges deeper aquifers, however, by how much is hard to estimate and requires more knowledge on the local hydrogeology.

The best simulated infiltration rate (K_res) was 0.067 mm $hour^{-1}$ (1,6 mm/day). This value falls within the infiltration rate range (0.1 – 4.9 mm day^{-1}) that was opposed by Fowe et al. (2015). They obtained an infiltration rate of 0.0088 mm $hour^{-1}$ (2.1 mm day^{-1}) of the Boura reservoir in Southern Burkina Faso.

The infiltration rate is subject to change in the course of time because of deposits of fine granular materials, which are carried to the reservoir by runoff from the catchment and reservoir banks. It is likely that the effective hydraulic conductivity of the reservoir bottom will decrease over time causing infiltration losses to be reduced.

4.5.4 Discharge

The reservoir discharges water from the spillway in the rainy season. In 2012 and 2015 the highest discharge volumes were simulated. In 2012 and 2015 the reservoir discharged, respectively, 3.2 MCM and 1.0 MCM water within the two months August to September. In the other years, the discharged ranged between 0.1 and 0.3 MCM. The significantly higher discharge in 2012 and 2015 compared to the other years can be attributed to the high total rainfall in August during those months (see figure 13). In 2012 the total amount of rainfall in August was 328 mm, with a maximum daily rainfall of 91 mm/day, and in 2015 the total amount

of rainfall in August was 412 mm, with a maximum daily rainfall of 76 mm/day. In the other years, the monthly rainfall in August was less than 228 mm.

4.5.5 Summary of the reservoir water balance

In figure 32 and table 13, the monthly and annual volumes of the water balance components are shown respectively. In the rainy season the reservoir fills up and reaches its maximum storage capacity within the months August and September, causing water to be discharged by the spillway during one or two months. Overland runoff and groundwater represent, with 79%, the major part of the average annual reservoir inflow, while direct rainfall on the reservoir contributes with 20% to the total inflow. The residual factor, i.e. indefinable water inflow, was 1% of the total inflow.

In the dry season the reservoir empties, due to major losses by evaporation (43%), infiltration (22%), and water consumption (13%). Reservoir storage has not fallen to critical volumes (<0.125 MCM). The lowest recorded reservoir storage, since the start of the measurements, was 1.37 MCM at the end of the dry season in 2012. Discharge was 10% of the average annual outflow. The residual factor, i.e. undefinable water outflow, was 1% of the total outflow.

The reservoir was not over-allocated or under stress during the past five years. The final- to initial-volume ratios in table 13 indicate that water is withdrawn from the reservoir at a sustainable rate i.e., the reservoir is not emptying.

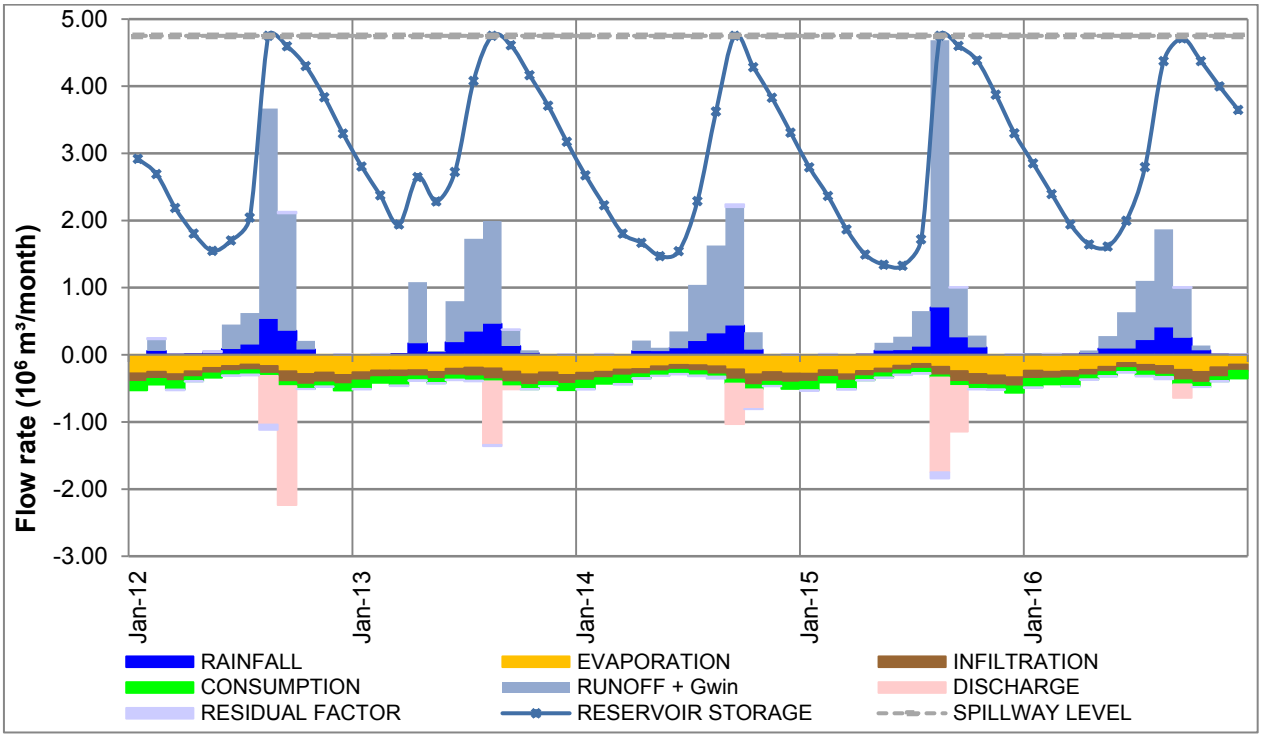

Figure 32: Monthly water balance of the Tandjari reservoir from 2012-2016.

Table 13: Annual water balance components [10^6 m^3] from 2012 to 2016

	2012	2013	2014	2015	2016	Average
Runoff and groundwater inflow	6,02	4,74	4,62	5,74	4,00	5,02
Direct rainfall	1,32	1,37	1,25	1,33	1,17	1,29
Annual total inflow	**7,33**	**6,11**	**5,87**	**7,07**	**5,17**	**6,31**
Evaporation	-2,83	-2,91	-2,64	-2,89	-2,39	2,73
Consumption	-0,79	-0,78	-0,79	-0,91	-0,96	-0,85
Infiltration	-1,39	-1,51	-1,34	-1,35	-1,41	1,40
Discharge	-2,49	-0,99	-0,90	-2,09	-0,20	1,33
Annual total outflow	**-7,51**	**-6,19**	**-5,67**	**-7,23**	**-4,95**	**-6,31**
Initial reservoir storage		3,3	3,2	3,3	3,3	3,27
Final reservoir storage	3,3	3,2	3,3	3,3	3,6	3,34
Ratio final/initial reservoir storage		**0,96**	**1,04**	**1,00**	**1,11**	**1,03**

* Residual factors, i.e. undefinable water inflow and outflow, were respectively 1% of total inflow and outflow.

4.5.6 Results climate and water demand scenario analysis

The scenario analysis was based on the worst historical drought since the start of the measurements in Fada N'Gourma in 1984 and additional adverse effects of climate and water demand changes. Table 14, shows the rainfall input for the different scenarios. The WXGEN program generated a drought period from 2029 to 2031 when annual rainfall input is predicted to be less than 700 mm.

Table 14: Annual rainfall input for the future reservoir simulations

Year	Annual rainfall (mm)	
	Baseline/D	CC/DCC
2027	922	879
2028	966	924
2029	612	577
2030	724	697
2031	559	520
2032	684	647
2033	973	925
2034	843	801
2035	792	752
2036	834	796
2037	932	890

The future reservoir balance is simulated over a period of ten years, from 2027 to 2037. The monthly reservoir storage under the different scenarios is presented in figure 33. In the baseline scenario, average annual reservoir storage was 2.89 MCM (table 15). The storage remained above the critical volume of 0.125 MCM at all times, which means all activities were supported

by sufficient water availability. The reservoir storage under scenario CC remains just above critical level, although the reservoir storage in May 2032 of 0.17 MCM got close to the critical volume. Hence, the ONEA could have continued its water withdrawal if this scenario would occur. Scenario D, on the other hand, would be disastrous as all water users would suffer from a dried up reservoir during a total of six months, which would occur in dry seasons of 2032 and 2033. The average annual reservoir storage was 18% less compared to the baseline scenario. In the final and worst case scenario, which included climate and water demand changes, the annual reservoir storage decreases with 32% compared to the baseline scenario. The critical level exceeds in three of the ten years and in 2032 and 2033 the reservoir would be dry for a total of nine months. Under this scenario there would be no discharge by the water spillway in six out of the ten years. The water shortage during these months would adversely affect local residents who depended on this resource.

Table 15: Mean annual quantities under different scenarios [10^6 m^3] of inflow, outflow, reservoir storage, and no spill years of the Tandjari reservoir from 2027 to 2037. Between brackets the % changes compared to the baseline simulation.

Scenarios	Inflow		Outflow		Reservoir storage		No spill years
Baseline	0,51		0,51		2,89		4
D	0,50	(-2%)	0,50	(-2%)	2,44	(-18%)	5
CC	0,45	(-13%)	0,46	(-12%)	2,62	(-10%)	5
DCC	0,44	(-16%)	0,45	(-14%)	2,18	(-32%)	6

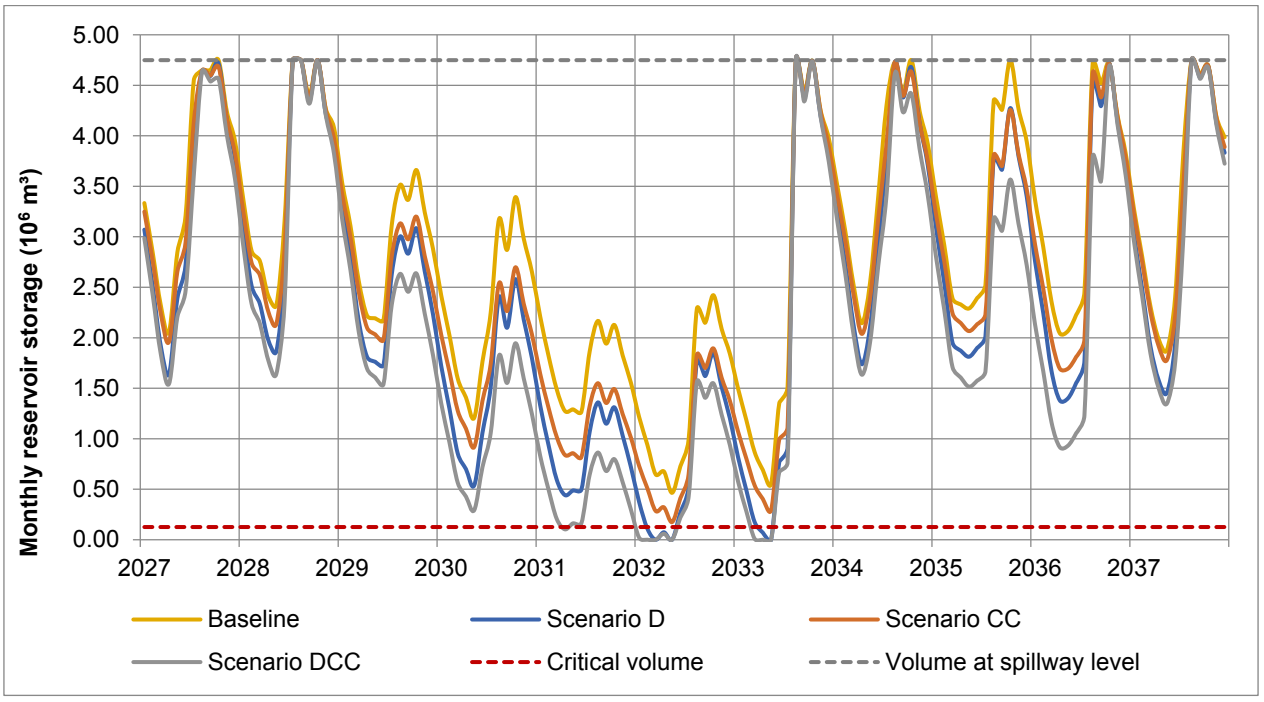

Figure 33: Future water balance simulations under different scenarios from 2027 to 2037

5 Discussion

On the left photo an employee of the Agence de l'Eau du Gourma is explaining an evaporation measurement to local residents. The right photo shows a reading being taken from the Mariotte bottle during an infiltration experiment, which was conducted by the author. Photos were taken by F. van Broekhoven on June 1, 2016

5 Discussion

It should be noticed that although comprehensive model calibration and validation were carried out, it does not guarantee reliability of the model predictions. The parameter values obtained with calibration and the results of the calibrated model are as realistic as the validity of the model assumptions for the Tandjari watershed and the quality and quantity data that were used for calibration and validation. The importance of data quality is reflected by the improved model performance for the validation period compared to the calibration period, for which different datasets were used. The difference between the datasets was largely determined by the location; the private station was situated more closely to the center of the catchment area what made recordings more reliable, in particular rainfall. The best simulation fitted the observed reservoir storage reasonably well and the model performance parameters give overall satisfactory results. However, a longer time period for validation, preferably two reservoir cycles, would be better.

The water balance simulations on a monthly scale have given a good understanding of the quantities and dynamics of the reservoir water balance. Runoff in the catchment upstream of the reservoir contributes most to the reservoir's inflow. Evaporation is a major factor of storage loss. Major evaporation loss was also identified at the Boura reservoir in Southern Burkina Faso by Fowe et al. (2015). In their paper they pointed out that the large evaporation potential makes shallow reservoirs less efficient compared to deep reservoirs. Infiltration is sometimes disregarded in reservoir water balance calculations because it is considered difficult to estimate or to measure (Andreini, 2016). However, the infiltration accounting for 22% of the total water outflow highlights the significance of this component. It was attempted to obtain an effective hydraulic conductivity of the reservoir bottom (K_{sat}) by infiltration measurements. However, with a lack of confidence in the obtained value (0.9 mm/h), it was chosen to optimize this parameter in the model calibration. The best simulated K_{sat} value (0.07 mm hour^{-1}) was 92.2% lower than the effective $K_{sat,}$ obtained by the measurements. The value of 0.07 mm hour^{-1} is in line with the findings of Fowe et al. (2015). Due to the large deviation between both results, the procedure, to estimate the infiltration capacity of the reservoir bottom, based on 4 infiltration measurements at different locations along the reservoir's shore, can be questioned. The infiltration capacities at locations along the shore, where perhaps the fraction of sand is higher, could vary much from infiltration capacities at the deeper bottom of the reservoir, where the fraction of clay in the soil is probably higher. Also mud cracks, which result in macro pores with enhanced infiltration flow, could have impacted the infiltration experiment.

Storage capacities of reservoirs in sandy areas are likely to decrease throughout the years on the account of sedimentation. Model simulations of the Tandjari reservoir are based on bathymetry data from 2014. The model parameters, which control the sedimentation rate of the reservoir, were set to default values and left uncalibrated due to a lack of observed data. If at all, it is expected that calibration of these parameters would have a minor influence on the results of the simulation from 2012 till 2017. However, calibration parameters for sediment are expected to have a significant importance on the results of the future scenario analysis. Therefore, caution is recommended when interpreting the results in detail regarding the future analysis. Calibration of

the sediment yield could have both a positive or negative effect on the future water availability of the Tandjari reservoir.

6 Conclusions

On the photo Frank van Broekhoven is explaining the functioning of a V-notch weir to employees of the Agence de l'Eau du Gourma. Photo taken by J. Stoffels on May 25, 2016

6 Conclusions

The main objective of this study was to determine the reservoir water balance of the Tandjari reservoir and the secondary objectives were to enhance knowledge on relevant input parameters for a hydrologic model, trend analysis of water utilization, and the impact of possible climatic and water demand changes.

By applying the distributed hydrologic model "Soil and Water Assessment Tool" (SWAT) the water balance components were quantified. The water balance over the past five years (2012-2016) showed that in the rainy season the reservoir fills up and reaches its maximum storage capacity within the months August and September, causing water to be discharged by the spillway during one or two months. On average 10% of the outflow was caused by discharge. Mean annual overland runoff, represented with 79%, the major part of the average annual reservoir inflow, while direct rainfall on the reservoir contributed with 20% to the total inflow. In the dry season the reservoir empties, due to major losses by evaporation (43%), infiltration (22%), and water consumption (13%). The general trend in reservoir water utilization shows that by far most water was withdrawn by the drinking water company (69%) for the water supply to residents in Fada N'Gourma, followed by irrigation water for agriculture (27%) and finally water withdrawals by local residents and livestock (3%). Reservoir storage has not fallen to critical volumes (<0.125 MCM). The lowest recorded reservoir storage, since the start of the measurements in 2012, was 1.37 MCM at the end of the dry season. This means that the reservoir was not over-allocated or under stress during the past five years. The average final-to initial-volume ratio of 1.03, indicates that water is withdrawn from the reservoir at a sustainable rate i.e., the reservoir is not emptying. However, climate change and increasing water demands ask for careful monitoring of the water balance. As the demand gets doubled by 2030, it is expected that during dry years (<700 mm annual rainfall) the reservoir cannot meet the water demand with the risk that the reservoir empties during the dry season. Climate change could have a worsening effect if the frequency and intensity of droughts will increase. The interruption of water withdrawals over a long period will adversely affect local residents who are depended on this resource.

For this study the distributed hydrologic model "Soil and Water Assessment Tool" (SWAT) was preferred over the set-up of a spreadsheet model, a model in numerical computing environment like Matlab, and other distributed hydrologic models, because 1) it is open source software that runs on a Geographical Information System (GIS) interface which allows GIS specialists in Burkina Faso to use the model; 2) the model can be supplemented with built-in data that comes with the SWAT installation which makes it useable in a study area for which limited data is available; 3) the SWAT model incorporates a rainfall-runoff method (SCS Curve Number method) that allows calculating runoff based on daily rainfall recordings 4) it has the advantages that it can be extended for modelling sedimentation, agricultural management, stream routing and water quality.

The model requires essential input data including a digital elevation raster, digital soil map with corresponding soil parameters (since these are not available in the model's integrated soil database for other than USA soils), a digital land cover map, weather statistics (including

rainfall, maximum and minimum temperatures), bathymetric data, and information on how reservoirs are operated. The NASA Shuttle Radar Topography Mission provides digital elevation data, the Agence de l'Eau du Gourma (AEG) produces soil and land cover maps, soil data can be obtained from the database of GEeau, which can be assessed at the website www.ge-eau.org, weather data can be requested by the National Meteorological Institute of Burkina Faso (DGM), and bathymetric and management data of some reservoirs can be requested by the National Office for Water and Sanitation (ONEA). As for the acquisition of data for calibration of the model; observed reservoir water levels, streamflow of ephemeral streams upstream of the dam, and reservoir discharge observations can be used.

The calibration and validation results show that the model was able to represent the reservoir water balance reasonably well. The acceptable model performance is reflected by the values of the Kling-Gupta efficiency (KGE) and the coefficient of determination (R^2), which were respectively 0.83 and 0.70 for the calibration period. The model simulations fitted the observed reservoir behavior generally well, apart from a mismatch in March 2013 when the model simulated an increase of reservoir storage, while the observations showed a decline in reservoir storage. The model showed a response to a localized rain event, which was captured by the rain gauge in Fada N'Gourma (DGM station), which did not occur in the Tandjari catchment. The PBIAS value of -0.0 % for the calibration period indicated that the model did not over- or underestimate the observed reservoir storage. The validated model showed that 75% of simulated data were bracketed by the 95PPU band and the thickness of the band, indicated by the R-factor, was 0.44. The KGE and R^2 of the validated model were respectively 0.78 and 0.93. The improved behavioral parameters for the validated model indicate an improvement of the model reliability by using a dataset that was obtained from a weather station, which had a better location with respect to the catchment. Moreover the observed reservoir data used in the validation procedure were obtained by automated water level recordings instead of manual readings, which minimized bias due to human intervention.

7 Recommendations

A fisherman checking his catch. Photo taken by the author on May 24, 2016

7 Recommendations

The recommendations in this chapter should provide guidance for the further development and improvement of hydrologic system analysis of reservoirs and their upstream catchments. Based on the conclusion of this study the following recommendations are formulated:

- The complexity of the SWAT model could be regarded as a limitation. It requires knowledge on hydrologic processes, basic experience with GIS and endurance to understand the model performance. However, the well documented user manual and numerous peer-reviewed articles that describe applications of SWAT help to enhance these skills. Table 16 presents guidelines for various monitoring methods that help to collect input data and data for calibration and validation of comprehensive hydrologic models, like SWAT.

Table 16: Guidelines for reservoir monitoring

Observations	Collection method and number of observations	Frequency	Purpose
Rainfall	Automated continuous (weather station, 1) and manual (gauge, 2)	Monthly readout of weather station and daily observations of rain gauges in rainy season (manual)	Input for hydrologic model and analysis
Weather parameters (solar radiation, wind speed, temperature, relative humidity)	Automated. Equipping the station with a radiation- and UV-sensor is recommended	Monthly readout of weather station	Input for hydrologic model
Reservoir water level	Automated (diver + baro diver, 1) and manual (staff gauge, 1)	Monthly readout of divers (hourly time interval divers), and monthly readings of staff gauge	Calibration of hydrologic model
Discharge spillway	Manual (staff gauge, 1). QH-relation required	Daily during discharge	Calibration of hydrologic model
Streamflow of (3) main ephemeral streams to reservoir (optional)	Manual (staff gauge, 3). QH-relation required	Daily during rainy season	Calibration of hydrologic model
Data on water consumption by people and livestock	Field observations, interviews with local residents, retrieval of statistical data*	Annually reported	Input for hydrologic model and analysis

**Statistical data from Central Office of the census, Provincial Department of Animal Resources, Provincial Department of Agriculture*

- This study relied on the bathymetric survey data that was available for the Tandjari reservoir. These surveys are expensive and hence only done for important and relative large reservoirs. However, smaller un-surveyed reservoirs are important too, since local communities rely heavily on them. “Regional area-volume equations have been developed for various regions in Africa i.e., northern Ghana (Liebe et al., 2005; Annor et al., 2009). Nothern Côte d’Ivoir (Cecchi, 2007), Botswana (Meigh,1995), and southern Zimbabwe (Sawunyama et al., 2006)”, but not for the Gourma region in Burkina Faso according to Liebe et al. (2009). It would therefore be valuable to develop a tailor-made area-volume equation, which enables models to be set-up for un-surveyed reservoirs.
- As demand and the frequency and intensity of anomalies such as droughts increases, an interruption of water withdrawals over a long period is inevitably. It will adversely affect local residents who are depended on this resource. Expanding reservoir storage by raising the spillway level or deepening the reservoir would not be sufficient for the anticipated water demand in 2030 because the maximum capacity of the reservoir is not utilized during consecutive years of drought. In this situation, importation of additional supplies from an outside source could be a solution. If there are no other sources that can meet the demand, the alternative would be to adapt the demand to meet the availability i.e. supply management. This is achieved by restricting the demand whenever the volume reaches critical levels. It is recommended to have a water regulation plan ready for such worst-case scenarios. To that end, water uses should be prioritized, taken into account health and food security.

Acknowledgements

This research project has been made possible by various organizations and people. By these acknowledgements I would like to show my gratitude to all of them.

First of all I want to thank my supervisors Piet Johan Radsma and Joost Stoffels who have entrusted me with this project and prepped me for the mission. I want to thank Paul Schot for being enthusiastic and supportive about the project and for supervising me in writing my thesis.

Key facilitators have been the Office National de l'Eau et de l'Assainissement (ONEA), the Direction Générale de la Météorologie du Burkina (DGM), Joost Wellens and Olivier Chanoine. Thank you for providing essential data for this research.

Last but not least I am very grateful to Frank van Broekhoven for being my dedicated companion on this mission and to all employees of the Agence de l'Eau du Gourma for; their very kind hospitality, facilitating the fieldwork and making this a rewarding and unforgettable Burkinabé experience.

Annex 1 Physical processes that drive infiltration

The forces that cause water to infiltrate into the soil are gravity, capillarity, adsorption and osmosis. These forces are often described in terms of energy. Water contains mechanical energy, which is called total water potential in the unsaturated zone. The total potential consists of gravitational potential and matric potential. Capillary forces and osmosis act as matric forces to the soil water. Osmotic potential is a negative force that draws water into the soil and reduces the mechanical energy. It is caused by differences in solute (ion) concentration in the soil, particular in salty soils (Hendriks, M. 2010).

The infiltration rate depends on the hydraulic conductivity of the soil. The hydraulic conductivity (k) is dependent on the moisture content of the soil. The dryer the soil is, the lower the hydraulic conductivity. The maximum hydraulic conductivity is reached at saturation of the soil (Hendriks, M. 2010).

During infiltration, the infiltration capacity of a soil decreases over time according to the infiltration curve, as illustrated in figure 1. The initial infiltration capacity in dry soils is high, because the matrix suction of the soil is large. In the near-saturated zone, the potential differences are less. At this point the soil moisture hardly causes any variance in matrix suction. Therefore, the infiltration capacity usually decreases within a couple of hours until it reaches a constant value that is almost equal to the saturated hydraulic conductivity. It should be noted that air bubbles during infiltration process prevents maximum saturation (Eijkelkamp, 2012). Table 2 gives an indication of the hydraulic conductivity for typical soil types.

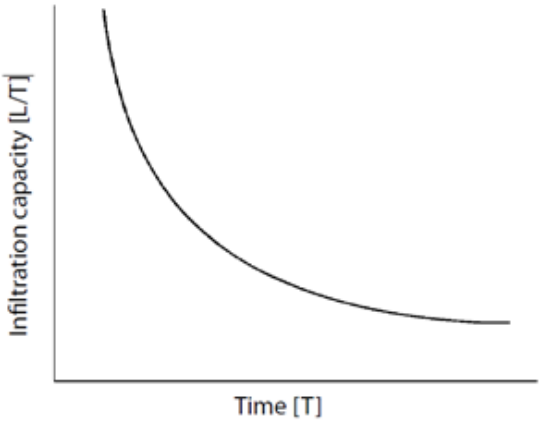

Figure 1: Course of infiltration in time

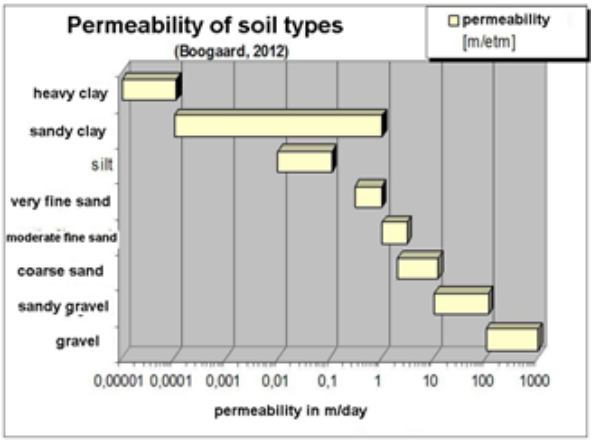

Table 2: permeability of soil types, after Boogaard, 2012.

Annex 2

Background on the reservoir area-volume relation in SWAT

SWAT creates an area volume equation based on two reservoir levels. The four values that the model need as input are the surface area and the volume when the reservoir is at normal level (during the dry season) and the same two values when the reservoir is at its maximum level (shortly after the rainy season). SA_{max} and V_{max} are respectively the surface area and the volume of water held in the reservoir at normal reservoir water level and SE_{nor} and V_{nor} are respectively the surface area and the volume of water held in the reservoir at maximum reservoir water level. Based on these input SWAT calculates the exponent *expsa* and the coefficient β_{sa}:

$$expsa = \frac{log_{10}(SA_{max}) - log_{10}(SA_{nor})}{log_{10}(V_{max}) - log_{10}(V_{nor})} \quad (7)$$

$$\beta_{SA} = \frac{SA_{em}}{(V_{em}{}^{expsa})} \quad (8)$$

With the above-calculated exponent and coefficient the surface area (SA) of the reservoir can be updated in time using the following formula:

$$SA = \beta_{sa} * V^{expsa} \quad (9)$$

Based on the results of a bathymetric survey of the Tandjari reservoir that is carried out in March 2014 by Serein-ge and the ONEA the values SA_{max}, V_{max}, SE_{nor}, V_{nor} are calculated.

Annex 3 Background on the Curve Number method in SWAT

The CN-model is an *empirical model* that calculates the runoff for a given rainfall depth based on Curve Numbers. It is an empirical formula based on several years of rainfall and runoff data obtained from a variety of combinations of soil, land cover, topography and climate across the US. The CN is related to the land cover and the soil hydrologic group (Ponce and Hawkins, 1996). The surface runoff is related to the rainfall depth and the retention parameter *S*. The initial abstraction, which is dependent on surface storage, interception and infiltration prior to runoff, is commonly approximated as 0.2S, which results in the following equation:

$$Q_{surf} = \frac{(P - 0.2S)^2}{P + 0.8S} \tag{10}$$

Where Q_{surf} is the accumulated runoff, *P* is the daily rainfall and *S* the retention parameter (mm water). *S* is calculated based on the curve number CN by the formula:

$$S = 25{,}4\left(\frac{1000}{CN} - 10\right) \tag{11}$$

The SCS defines three antecedent moisture conditions; dry (wilting point), average moisture and wet (field capacity). The curve number for the three antecedent conditions can be calculated by a formula that is not discussed here.
Runoff occurs when the rainfall is greater than the initial abstraction, which is assumed to be 20% of the curve number value.

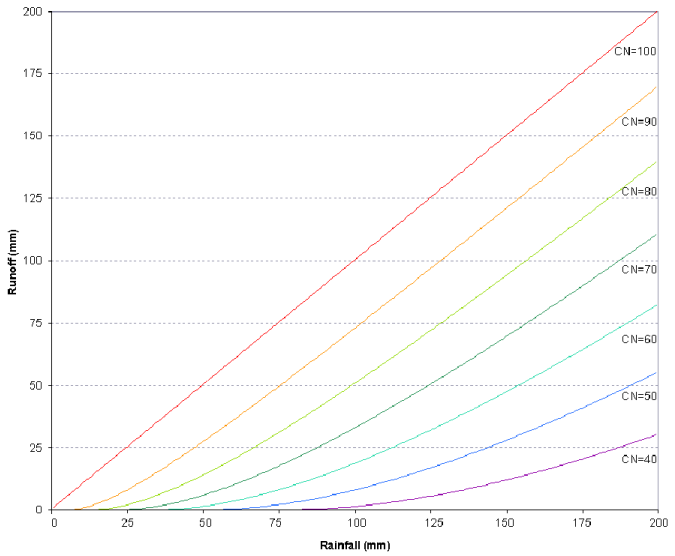

Figure 1: relationship between runoff and rainfall and the related Curve Numbers (Neitsch et al., 2009)

SWAT allows selecting between two methods to calculate the retention parameter *S*. The traditional method of the parameter varying with the soil profile water content or the method where *S* varies with accumulated plant evapotranspiration. For this research the traditional method is applied.
The inflow of water in the reservoir (V_{RO}) is the fraction of water of the catchment area that drains into the reservoir. The catchment area is fed by excess water after a rain event that flows from the highest elevations in the catchment area to the reservoir (lowest elevation). The contributing area increases with the size of the storm (Liebe *et al.,* 2009).
The fraction of water that drains into the reservoir can be subdivided in groundwater flow, lateral flow and surface runoff.

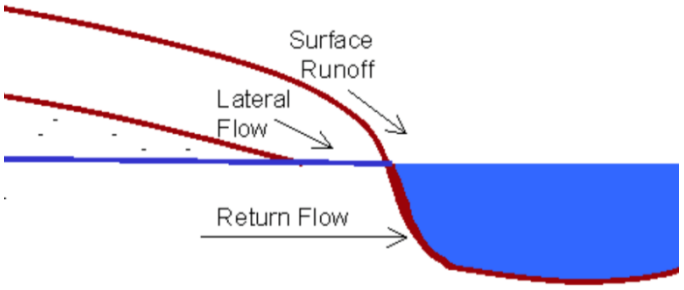

Figure 2: Sub flows of water into a reservoir (after Neitsch et al., 2002).

Based on the HRU's the sub flows are calculated. Based on these sub flows the total inflow of water into the reservoir (V_{inflow}) is calculated, by the following formula:

$$V_{in} = fr_{imp} * 10 * \left(Q_{surf} + Q_{gw} + Q_{lat}\right) * (Area - SA) \quad (12)$$

Where Fr_{imp} is the fraction of the catchment area draining into the reservoir, Q_{surf} is the surface runoff from the catchment area (mm H2O), Q_{gw} is the groundwater flow from the catchment area, Q_{lat} is the lateral flow generated in a catchment area. The term 'area' is the water catchment area (ha), and SA is the surface area of the reservoir (ha) (Neitsch *et al.,* 2002).

Annex 4
Background on rainfall and evaporation calculations in SWAT

Rainfall data

Rainfall that falls directly on the reservoir by a given day is calculated with the following formula:

$V_{pcp} = 10 * R_{day} * SA$

where V_{pcp} is the volume of water added to the reservoir by rainfall, R_{day} is the amount of rainfall falling on a given day (mm) and SA is the surface area of the water body (ha).

Evaporation data

In order to know the volume of water lost due to evaporation (V_e) the open-water evaporation rate needs to be known (m^3 H_2O). This is the rate of water transformation to vapor from open water (mm day^{-1}) from the reservoir and can be calculated by knowing the surface area (SA) of the reservoir (ha), the open water evaporation rate (E_o) (mm H_2O) and a conversion factor, hereafter called the evaporation coefficient (η), using the formula:

$V_{evap} = 10 * \eta * E_o * SA.$

The evaporation coefficient is usually a value between 0.6 and 0.7 (Linacre, E., & Geerts, B. 1997; Neitsch *et al.,* 2002). Based on a literature review the appropriate coefficient will be selected. The National Meteorological Institute (Agence Nationale de La Météorologie) has made available daily evaporation data from the meteorological service in Fada N'Gourma over the period from 1984 to 2015. The evaporation is measured with an (US Weather Bureau Class A) evaporation pan. In the absence of rain, the amount of water evaporated from this pan during a period corresponds with the decrease in water depth in that period. The measurement integrates the effects of radiation, wind, temperature and humidity on evaporation from an open water surface. However the evaporation from this type of pan will generally be higher than the open-water evaporation due to the warming effect of the sides of the pan by solar radiation. To compensate for this effect it is usual to use a pan coefficient. The coefficients for this type of pan range from 0.35 to 0.85 depending on relative humidity, wind speed, and the length of the upwind distance of green crop or dry fallow (Doorenbos and Pruitt 1977). The site-specific coefficient is determined from the table presented in appendix 2 of the FAO irrigation and Drainage Paper No. 24. A value of 0.75 has been found to be best applicable in this situation. Because a screen is mounted over the pan which has a lowering effect on the evaporation, the pan coefficient is increased with 5% resulting in a final coefficient of 0.8 (Doorenbos & Pruitt, 1977).

Annex 5 Evaporation pan coefficients

Pan coefficients (K_p) for Class A pan for different pan siting and environment and different levels of mean relative humidity and wind speed (FAO Irrigation and Drainage Paper No. 24)

Class A pan	**Case A: Pan placed in short green cropped area**				**Case B: Pan placed in dry fallow area**			
RH mean (%) →		**low < 40**	**medium 40 - 70**	**high > 70**		**low < 40**	**medium 40 - 70**	**high > 70**
Wind speed (m s^{-1})	**Windward side distance of green crop (m)**				**Windward side distance of dry fallow (m)**			
Light	1	.55	.65	.75	1	.7	.8	.85
< 2	10	.65	.75	.85	10	.6	.7	.8
	100	.7	.8	.85	100	.55	.65	.75
	1000	.75	.85	.85	1000	.5	.6	.7
Moderate	1	.5	.6	.65	1	.65	.75	.8
2-5	10	.6	.7	.75	10	.55	.65	.7
	100	.65	.75	.8	100	.5	.6	.65
	1000	.7	.8	.8	1000	.45	.55	.6.
Strong	1	.45	.5	.6	1	.6	.65	.7
5-8	10	.55	.6	.65	10	.5	.55	.65
	100	.6	.65	.7	100	.45	.5	.6
	1000	.65	.7	.75	1000	.4	.45	.55
Very strong	1	.4	.45	.5	1	.5	.6	.65
> 8	10	.45	.55	.6	10	.45	.5	.55
	100	.5	.6	.65	100	.4	.45	.5
	1000	.55	.6	.65	1000	.35	.4	.45

Annex 6 Survey sheet on water consumption

Fiche enquête sur les prélèvements d'eau
Date: 17-06-2016

What is the total number of cattle (cows/sheep/goats) that use the reservoir for drinking?

Avez-vous une idée du nombre total de bovins (vaches / ovins / caprins) qui s'abreuvent au niveau du barrage de Tandjari?

Bongo Adjina, Komandougou
60.000 (total in catchment)

Lompo Ladja, Tankilounga
50.000

Thomas Woba, Tandjari
50.000

Vaches : 1
Caprins (Chevre): 20
Mouton (Ovin) : 10
Caprins : 2

Donkeys only used for work (1 per family)
Goat fast reproducing (3 to 4 baby's)
Sheep pretty fast reproducing (1/2 baby's)

Note: Peul are nomads and have no permanent residence. They live from livestock. Animals or meat are traded for other food and goods. On average 50 to 100 cows in a herd.

How many times per week do the cows/sheep/goats come to drink at the reservoir?

Combien de fois par semaine viennent boire les vaches / moutons / chèvres au barrage de Tandjari?

Bongo Adjina, Komandougou
Trois fois

Lompo Ladja, Tankilounga
Trois fois

Thomas Woba, Tandjari
Trois fois

Do you know roughly how much water an adult cow drinks a day?

Savez-vous à peu près quelle quantité d'eau peut boire une vache par exemple en un jour?

Bongo Adjina, Komandougou
Vache: 25 L/ deux fois

Lompo Ladja, Tankilounga
25 – 75 L

Thomas Woba, Tandjari
25 L deux fois par jour

Depending on the season (dry/wet)

Is water from the reservoir used for brick making? If yes, how much water is approximately used?

Y a t-il des briquettiers au niveau de ce barrage ? Si oui, quelle quantité d'eau prélève t-il en moyenne par jour?

Bongo Adjina, Komandougou
20 bariques / jour. Pour une maison de ..

Lompo Ladja, Tankilounga
-

Thomas Woba, Tandjari
Oui

5 bariques par maison et 15 bariques pour usage domestic.

Is water from the reservoir used for irrigation? If yes, how often and how much water is abstracted?

L'eau du barrage de Tandjari est-elle utilisée pour l'irrigation? Si oui, à quelle fréquence et quelle quantité prélevée?

Bongo Adjina, Komandougou
2 heur/jour moto pumpes

Lompo Ladja, Tankilounga
Deux ou trois jours par semaine at max 3 heurs

Thomas Woba, Tandjari
Tout les jours ~ 3 h

Do tank trucks abstract water from the reservoir? If yes, how often and much water is abstracted?

Ya-t-il des camions-citernes qui prélèvent l'eau de ce barrage? Si oui, à quelle fréquence et quelle est la quatité prélevée?

Bongo Adjina, Komandougou
-

Lompo Ladja, Tankilounga
En ces de travaux, mais sera?
Avec taxi-moto 4 barriques

Thomas Woba, Tandjari
-

What is the population of the village ? How many families does live here?

Pouvez-vous nous donner une estimation de la population du village? Combien de ménages environ habite ici?

Bongo Adjina, Komandougou
51 concessions

Lompo Ladja, Tankilounga
30 concessions

Thomas Woba, Tandjari
21 concession

Is there a groundwater pump near the village that is been used?

Y a t-il un forage dans ce village?

Bongo Adjina, Komandougou
Non

Lompo Ladja, Tankilounga
Une forage

Thomas Woba, Tandjari
Non

Bibliography

Abbaspour, K. (2015). SWAT-Calibration and uncertainty programs (CUP). *Neprashtechnology.Ca*. https://doi.org/10.1007/s00402-009-1032-4

Adjina, B., personal communication, Komandougou, June 17, 2016

Agence de l'eau du Gourma (AEG) (2014). Retrieved March 2016. http://www.eaugourma.bf/?lang=en

Allen, M. R., Barros, V. R., Broome, J., Cramer, W., Christ, R., Church, J. A., ... & Edenhofer, O. (2014). IPCC fifth assessment synthesis report-climate change 2014 synthesis report.

Andreini, M. (2016). Small reservoir project. Retrieved March 2016. http://www.smallreservoirs.org/

Boelee, E., Cecchi, P., & Koné, A. (2009). Health Impacts of Small Reservoirs in Burkina Faso. Working Paper No. 136. Colombo, Sri Lanka: International Water Management Institute.

Bosilovich, M. G., & Authors, V. (2007). MERRA-2: File Specification. *Earth*, *9*(9), 0–1.

Chanoine, O., Expert infrastructures, Sector and Thematic Expertise Department at Belgian Development Agency (BTC). Personal communication (December 6, 2016)

Climatic Research Unit (CRU) of University of East Anglia (UEA), 2016. *Average Monthly Temperature and Rainfall at the Tandjari dam (lat.12.19, lon. 0.33) from 1990-2012.* Temperature data (CRUTEM4, HadCRUT4: 1850-present global data on a 5° x 5° grid). Rainfall data (Hulme dataset: global land data on 5°x5° and 2.5°x3.75° grids for 1900-1998). retrieved from http://sdwebx.worldbank.org/climateportal/index.cfm?page=country_historical_climate&ThisRegion=Africa&ThisCCode=BFA

Commonwealth of Australia. (2015). *Description of the water-dependent asset register for the Gloucester subregion*. Retrieved from http://www.bioregionalassessments.gov.au/assessments/13-water-dependent-asset-register-gloucester-subregion

Di Luzio, M., Srinivasan, R., Arnold, J.G., 2001. ArcView Interface for SWAT2000 – *User's Guide*. Blackland Research Center, Texas Agricultural Experiment Station and Grassland, Soil and Water Research Laboratory, USDA Agricultural Research Service, Temple,Texas.

Dingman, S. L. (2015). *Physical hydrology*. Waveland press.

Direction Générale de la Météorologie du Burkina (DGM) (2016). Database with meteorological parameters. The data originates from a weather station at the airport of Fada N'Gourma (12°02'44.8"N 0°21'52.2"E)

Doorenbos, J., & Pruitt, W. O. (1977). *Guidelines for predicting crop water requirements*. Food and Agriculture Organization of the United Nations, 154.

Eijkelkamp. (2015). Double Ring Infiltrometer Manual, 1–9.

Eilander, D. M. (2013). *Monitoring the Water Balance of Small Reservoirs in Semi-arid Regions ESA Alcantara Research Project* 12-A11 & TIGER P.308.

Elèves du LDM La Champagne de Vitré au LTO de Ouagadougou. (n.d.). Retrieved from http://elevesduldmlachampagnedevitreaultodeouagadougou.hautetfort.com/

Esri, HERE, DeLorme, Intermap, increment P Corp., GEBCO, USGS, FAO, NPS, NRCAN, GeoBase, IGN, Kadaster NL, Ordnance Survey, Esri Japan, METI, Esri China (Hong Kong), swisstopo, MapmyIndia, © OpenStreetMap contributors, and the GIS User Community (2016-1)

Esri, DigitalGlobe, GeoEye, Earthstar Geographics, CNES/Airbus DS, USDA, USGS, AeroGRID, IGN, and the GIS User Community (2016-2)

Forbes, T. R. (1973). Ferrallitic and ferruginous tropical soils of West Africa, *211*.

Gupta, H. V., Kling, H., Yilmaz, K. K., & Martinez, G. F. (2009). Decomposition of the mean squared error and NSE performance criteria: Implications for improving hydrological modelling. *Journal of Hydrology*, *377*(1–2), 80–91. https://doi.org/10.1016/j.jhydrol.2009.08.003

Gunasekara, N. K., Kazama, S., Yamazaki, D., & Oki, T. (2014). Water Conflict Risk due to Water Resource Availability and Unequal Distribution. *Water Resources Management*, *28*(1), 169–184. https://doi.org/10.1007/s11269-013-0478-x

Haas, S. (2010). *Hydrogeology and siting of micro-dams around Léo, Burkina Faso*.

Hendriks, M. (2010). *Introduction to physical hydrology*. Oxford University Press.

Howard, G., & Bartram, J. (2003). Domestic Water Quantity , Service Level and Health. *World Health Organization*, 39. https://doi.org/10.1128/JB.187.23.8156

Ibrahim, B., Polcher, J., Karambiri, H., & Rockel, B. (2012). Characterization of the rainy season in Burkina Faso and it's representation by regional climate models. *Climate Dynamics*, *39*(6), 1287–1302. https://doi.org/10.1007/s00382-011-1276-x

Institute National de la Statistique et de la Démographie (INSD) (2000*). Analyse des résultats du recensement général de la Population et de l'Habitation de 1996- Volume 1*. (English Edition), 374.

Jones, F. E. (1991). Evaporation of Water: with Emphasis on Applications and Measurements. Chelsea, Michigan: Lewis Publishers, Inc.

King, K. W., Arnold, J. G., & Bingner, R. L. (1999). *Comparison of Green-Ampt Mein-Larson and Curve Number methods on Goodwin Creek watershed Using Swat*. Transactions of the ASAE 1999, 42(2), 919–925. http://doi.org/10.13031/2013.13272

Lang, M., Wellens, J., & Tychon, B. (2011). ArcSWAT manuel d'utilisateur - Cas du bassin versant du Kou (Burkina Faso). Retrieved from http://www.ge-eau.org/

Lhoste, P., Dollé, V., Rousseau, J., & Soltner, D. (1993). *Zootechnie des régions chaudes: Les systèmes d'élevage* (2e edition).

Liebe, J. R., N. van de Giesen, M. Andreini, M. T. Walter, and T. S. Steenhuis (2009), Determining watershed response in data poor environments with remotely sensed small reservoirs as runoff gauges, Water Resour. Res., 45, W07410, doi:10.1029/2008WR007369.

Linacre, E., & Geerts, B. (1997). Climates and Weather explained. London: Routledge.

Lompo, L., Chief's agriculture's department, personal communication, Tankilounga, June 30, 2016

MacDonald, A. M., & Bonsor, H. C. (2011). *An initial estimate of depth to groundwater across Africa*. Groundwater Science Programme. Open Report OR/11/067, 26.

Ministère de l'Agriculture de l'Hydraulique et des Ressources halieutiques (MAHPH). (2009). Plan d'Action pour la Gestion Intégrée des Ressources en Eau (PAGIRE).

Ministère de la coopération et du développement. (1988). *Manuel Vétérinaire* (2e ed.).

Ministère de l'Eau Direction de l'Inventaire des Ressources Hydrauliques, & Iwaco. (1993). Carte Hyrdogeologique du Burkina Faso Carte Est.

Muleta, M. K., & Nicklow, J. W. (2005). Sensitivity and uncertainty analysis coupled with automatic calibration for a distributed watershed model. *Journal of Hydrology*, *306*(1–4), 127–145. https://doi.org/10.1016/j.jhydrol.2004.09.005

NASA Shuttle Radar Topography Mission (SRTM) and provided by the U.S. Geological Survey's (USGS) Long Term Archive (LTA) at the National Center for Earth Resource Observations and Science (EROS) in Sioux Falls (2015).

Neitsch, S.L, Arnold, J.G, Kiniry, J.R, & Williams, J.R. (2009). *Soil & Water Assessment Tool Theoretical Documentation Version 2009*. Texas Water Resources Institute, 1–647. http://doi.org/10.1016/j.scitotenv.2015.11.063

Ouessar, M., Bruggeman, A., Abdelli, F., Mohtar, R. H., Gabriels, D., & Cornelis, W. M. (2009). Modelling water-harvesting systems in the arid south of Tunisia using SWAT. *Hydrology and Earth System Sciences*, *13*(10), 2003–2021. https://doi.org/10.5194/hessd-5-1863-2008

Office National de l'Eau et de l'Assainissement (ONEA). (2015). Suivi-controle des travaux de rehabilitation du barrage de Tandjari, province du Gourma, region de l'Est.

ONEA. (2016). *Rapport Mensuel D'exploitation*.

Rosenberg, N. J., Blad, B. L., & Verma, S. B. (1983). Microclimate: the biological environment. John Wiley & Sons.

Sally, H.; Lévite, H. and Cour, J. 2011. Local water management of small reservoirs: Lessons from two case studies in Burkina Faso. Water Alternatives 4(3): 365-382

Schuol, J., and K. C. Abbaspour. "Calibration and uncertainty issues of a hydrological model (SWAT) applied to West Africa." Advances in geosciences 9 (2006): 137-143.

Schuol, J., Abbaspour, K. C., Srinivasan, R., & Yang, H. (2008*). Estimation of freshwater availability in the West African sub-continent using the SWAT hydrologic model*. Journal of Hydrology, 352(1–2), 30–49. https://doi.org/10.1016/j.jhydrol.2007.12.025

SEREIN-GE SARL (2014). ONEA *Rapport de realisation des travaux d'installation d'echelles limnimetriques et de leves bathymetriques et topographiques sur les barrages d'itengue, de salbisgo, de tandjari et de yakouta*

Sharpley, A.N., Williams, J.R. (Eds.), 1990*. EPIC-Erosion Productivity Impact Calculator, 1. Model documentation. US Department of Agriculture*, Agricultural Research Service, Tech. Bull.1768.

Smedema, L.K., Rycroft, D.W. 1983. Land drainage – planning and design of agricultural drainage systems, Cornell University Press, Ithica, N.Y.

Sougoulingo, S., personal communication, Komangou, June 22, 2016

Stackhouse, P. W. NASA Surface meteorology and Solar Energy: Daily Averaged Data. Retrieved March 2, 2017, from https://eosweb.larc.nasa.gov/cgi-bin/sse/daily.cgi?email=skip@larc.nasa.gov

United Nations Development Programme (UNDP). (2015). Human Development Report. *Work for Human Development*. https://doi.org/ISBN: 978-92-1-126398-5

Unité Progrès Justice (2011). Convention constitutive du groupement d'interet public

Wellens, J. (2016), University of Liège. Database with soil parameters based on soils in the Kou Watershed, West Burkina Faso.

WHO, & Unicef. (2000). Global Water Supply and Sanitation Assessment 2000 Report. *Water Supply*, 87. https://doi.org/http://www.who.int/water_sanitation_health/monitoring/globalassess/en/

Woba, T., personal communication, Tandjari , June 17, 2016

World Waternet. (2017). Burkina Faso: WOP Water Authority AEG - Wereld Waternet. Retrieved March, 2017, from http://www.worldwaternet.com/projecten/burkina-faso/wop-waterschap-aeg/

Zakarie, attendant of the pumping station at the water intake of the Tandjari dam, personal communication (December 24, 2016)